AFRL-RB-WP-TM-2008-3154

MORPHING AIRCRAFT STRUCTURES: RESEARCH IN AFRL/RB

Gregory W. Reich, Jason C. Bowman, Brian Sanders Matthew P. Snyder, Bryan Cannon, Franklin E. Eastep, Geoffrey J. Frank, Jayanth Kudva, Shiv Joshi , and Terrence Weisshaar

Advanced Structural Concepts Branch
Structures Division

SEPTEMBER 2008
Final Report

Approved for public release; distribution unlimited.

See additional restrictions described on inside pages

STINFO COPY

AIR FORCE RESEARCH LABORATORY
AIR VEHICLES DIRECTORATE
WRIGHT-PATTERSON AIR FORCE BASE, OH 45433-7542
AIR FORCE MATERIEL COMMAND
UNITED STATES AIR FORCE

NOTICE

Using Government drawings, specifications, or other data included in this document for any purpose other than Government procurement does not in any way obligate the U.S. Government. The fact that the Government formulated or supplied the drawings, specifications, or other data does not license the holder or any other person or corporation; or convey any rights or permission to manufacture, use, or sell any patented invention that may relate to them.

This report was cleared for public release by the Air Force Research Laboratory Wright-Patterson Air Force Base (WPAFB) Public Affairs Office and is available to the general public, including foreign nationals. Copies may be obtained from the Defense Technical Information Center (DTIC) (http://www.dtic.mil).

THIS REPORT HAS BEEN REVIEWED AND IS APPROVED FOR PUBLICATION IN ACCORDANCE WITH ASSIGNED DISTRIBUTION STATEMENT.

This report is published in the interest of scientific and technical information exchange and its publication does not constitute the Government's approval or disapproval of its ideas or findings.

*Disseminated copies will show "//signature//" stamped or typed above the signature blocks.

REPORT DOCUMENTATION PAGE			*Form Approved* *OMB No. 0704-0188*

The public reporting burden for this collection of information is estimated to average 1 hour per response, including the time for reviewing instructions, searching existing data sources, searching existing data sources, gathering and maintaining the data needed, and completing and reviewing the collection of information. Send comments regarding this burden estimate or any other aspect of this collection of information, including suggestions for reducing this burden, to Department of Defense, Washington Headquarters Services, Directorate for Information Operations and Reports (0704-0188), 1215 Jefferson Davis Highway, Suite 1204, Arlington, VA 22202-4302. Respondents should be aware that notwithstanding any other provision of law, no person shall be subject to any penalty for failing to comply with a collection of information if it does not display a currently valid OMB control number. **PLEASE DO NOT RETURN YOUR FORM TO THE ABOVE ADDRESS.**

1. REPORT DATE *(DD-MM-YY)* September 2008	2. REPORT TYPE Final	3. DATES COVERED *(From - To)* 10 December 2001 – 15 September 2008	

4. TITLE AND SUBTITLE MORPHING AIRCRAFT STRUCTURES: RESEARCH IN AFRL/RB	5a. CONTRACT NUMBER In-house
	5b. GRANT NUMBER
	5c. PROGRAM ELEMENT NUMBER 0601102
6. AUTHOR(S) Gregory W. Reich, Jason C. Bowman, Brian Sanders, and Matthew P. Snyder (Structures Division, Advanced Structural Concepts Branch (AFRL/RBSA)) Bryan Cannon (Control Sciences Division, Control Systems Development and Application Branch (AFRL/RBCC)) Franklin E. Eastep and Geoffrey J. Frank (University of Dayton Research Institute) Jayanth Kudva and Shiv Joshi (NextGen Aeronautics) Terrence Weisshaar (Purdue University)	5d. PROJECT NUMBER A01Y
	5e. TASK NUMBER
	5f. WORK UNIT NUMBER 0C

7. PERFORMING ORGANIZATION NAME(S) AND ADDRESS(ES) Advanced Structural Concepts Branch (AFRL/RBSA) Structures Division Air Force Research Laboratory, Air Vehicles Directorate Wright-Patterson Air Force Base, OH 45433-7542 Air Force Materiel Command, United States Air Force - Control Sciences Division, Control Systems Development and Application Branch (AFRL/RBCC) - University of Dayton Research Institute - NextGen Aeronautics - Purdue University	8. PERFORMING ORGANIZATION REPORT NUMBER AFRL-RB-WP-TR-2008-3154

9. SPONSORING/MONITORING AGENCY NAME(S) AND ADDRESS(ES) Air Force Research Laboratory Air Vehicles Directorate Wright-Patterson Air Force Base, OH 45433-7542 Air Force Materiel Command United States Air Force	10. SPONSORING/MONITORING AGENCY ACRONYM(S) AFRL/RBSA
	11. SPONSORING/MONITORING AGENCY REPORT NUMBER(S) AFRL-RB-WP-TR-2008-3154

12. DISTRIBUTION/AVAILABILITY STATEMENT
Approved for public release; distribution unlimited. Document contains color.

13. SUPPLEMENTARY NOTES
PAO Case Numbers: AFRL-WS-05-2806, 03 June 2005; AFRL/WS 06-0744; AFRL-WS 08-0860. © 2005, 2006, and 2007 AIAA. This work was funded in whole or in part by Department of the Air Force work unit A01Y0C. The U.S. Government has for itself and others acting on its behalf a paid-up, nonexclusive, irrevocable worldwide license to use, modify, reproduce, release, perform, display, or disclose the work by or on behalf of the U. S. Government. Published in AIAA 2005-1994, 46th AIAA/ASME/ASCE/AHS/ASC Structures, Structural Dynamics & Materials Conference, Austin, TX, 18-21 April 2005; AIAA 2006-6727, Proc. AIAA Modeling and Simulation Technologies Conference and Exhibit, Keystone, CO, 21-24 August 2006; AIAA 2007-1730, 48th AIAA/ASME/ASCE/AHS/ASC Structures, Structural Dynamics, and Materials Conference, Honolulu, HI, 23-26 April 2007. Report contains color.

14. ABSTRACT
This report reviews research in several different areas related to morphing aircraft structures undertaken in AFRL/RBSA. The first is an aeroelastic analysis of a folding-wing vehicle to determine the flutter boundaries of the wing at different fold angles. The second is the development of a simulation tool to study both the flight stability of a morphing vehicle during the morphing process, and the kinematic stability of the morphing mechanism subject to aerodynamic and inertial loads. The third is a series of first-order analyses to determine the system-level benefits of morphing at the mission, sortie, and campaign levels.

15. SUBJECT TERMS
Morphing aircraft, morphing wings, aeroelasticity, morphing simulation, morphing performance, morphing benefit

16. SECURITY CLASSIFICATION OF:			17. LIMITATION OF ABSTRACT: SAR	18. NUMBER OF PAGES 40	19a. NAME OF RESPONSIBLE PERSON (Monitor) Gregory W. Reich
a. REPORT Unclassified	b. ABSTRACT Unclassified	c. THIS PAGE Unclassified			19b. TELEPHONE NUMBER (Include Area Code) 937-255-3031

Standard Form 298 (Rev. 8-98)
Prescribed by ANSI Std. Z39-18

Executive Summary

This report reviews research in several different areas related to morphing aircraft structures undertaken in AFRL/RBSA. The first is an aeroelastic analysis of a folding-wing vehicle to determine the flutter boundaries of the wing at different fold angles. The second is the development of a simulation tool to study both the flight stability of a morphing vehicle during the morphing process, and the kinematic stability of the morphing mechanism subject to aerodynamic and inertial loads. The third is a series of first-order analyses to determine the system-level benefits of morphing at the mission, sortie, and campaign levels.

The flutter analyses characterize the dynamic aeroelastic aspects of a morphing aircraft design concept. The notion of interest is a folding wing that enables wing area changes on the order of 200%. A finite element approach is used to investigate the sensitivity of natural frequencies and flutter instabilities to the wing position (e.g., fold angle), actuator stiffness, and vehicle weight. Sensitivities in these areas drive design requirements and raise flight envelope awareness issues. Various discrepancies in the results are further analyzed for clarification.

The simulation tool combines aspects of the traditional static aeroelasticity analysis with transient multi-body dynamics simulations. It is based on a need for transient analysis of morphing vehicles. The result is a tool that can be used to study the flight control and mechanism stability of a free-flying morphing vehicle during morphing. Aerodynamic loads are computed at each time step based on current mechanism and flexible structure position and rates. Free flight is enabled by incorporation of a flight control model with inner- and outer-loop commands, meaning that particular maneuvers can be flown, or particular states can be achieved. Extensions to the code have been made for post-stall behavior, useful for MAVs. The code still lacks a time-dependent aerodynamic wake capability, which would be critical for use on flapping-wing and other highly transient behaviors.

For the system-level performance analysis, first-order calculations are made of mission segments to identify how a morphing vehicle would compare to a fixed-geometry vehicle subject to realistic geometric constraints. Additionally the benefits of morphing can be demonstrated by relating low-level metrics such as lift-to-drag ratio to system-level metrics which include life cycle cost, flyaway cost, cost per kill box, etc.

Vibration and Flutter Characteristics of a FoldingWing

Matthew P. Snyder[*] and Brian Sanders[†]
Air Force Research Laboratory, Wright Patterson Air Force Base, OH 45433 USA

Franklin E. Eastep[‡] and Geoffrey J. Frank[§]
University of Dayton Research Institute, Dayton, OH 45469 USA

Studies are presented that characterize the dynamic aeroelastic aspects of a morphing aircraft design concept. The notion of interest is a folding wing that enables wing area changes on the order of 200%. A finite element approach is used to investigate the sensitivity of natural frequencies and flutter instabilities to the wing position (e.g., fold angle), actuator stiffness, and vehicle weight. Sensitivities in these areas drive design requirements and raise flight envelope awareness issues. Various discrepancies in the results are further analyzed for clarification.

I. Introduction

The concept of wing shape control had its roots in the original flying machine. Consider the Wright brothers use of wing warping or twisting for flight control on the first flying machine. The shape control of the wing enabled Wilbur and Orville to control pitch, yaw, and roll rate of the aircraft. As one follows the evolution of the aircraft, however, fixed geometry, high stiffness wings emerge as the dominant trait. As a result, air vehicles are optimized for specific flight conditions, e.g., a commercial airliner is designed to be aerodynamically efficient for cruising long distances at a set speed and altitude. Flight dynamiscists realize changes in geometry could provide significant increases in flight efficiency, but technology has prohibited this becoming reality. Limitations exist due to structural design considerations; aeroelastic instabilities limiting the flight envelope, lack of actuator power for driving such designs, or skins not able to withstand strains imposed by actuation.

In an effort to exploit these concepts, the Defense Advanced Research Projects Agency, DARPA, Morphing Aircraft Structures (MAS) program is developing novel technology defined by the goal of utilizing radical wing shape changes to expand the flight envelopes and operational characteristics of flight vehicles. Morphing vehicles are classified as structures exploiting actuation mechanisms to achieve substantial shape change resulting in previously unachievable performance as demonstrated through interaction with diverse mission requirements. This involves the development and integration of advanced materials, actuation systems, mechanisms, and controls laws. The concept behind morphing vehicles stems from the desire to expand mission capabilities of aircraft platforms. Radical wing area changes would enable a single air vehicle to perform a variety of tasks normally involving multiple aircraft with varying missions. In age of unmanned aerial vehicles (UAV) human induced flight termination limitations are replaced by limitations such as range and engine performance. A morphing vehicle would help expand the range of a vehicle by increasing its mission segment efficiency. For example, the vehicle could cruise at an optimal configuration and then morph to an optimal dash configuration.

The DARPA MAS program is multi-phased due to the necessity of first developing the underlying technology necessary for a morphing vehicle. The radical changes in wing area described in this paper are the synthesis of materials and flexible structural components capable of maintaining aerodynamic shape while varying structural

---

[*] Adaptive Structures Engineer, AFRL/VASA, 2210 8th Street, Bldg 146, WPAFB, OH 45433, AIAA member.
[†] Senior Aerospace Engineer, AFRL/VASA, 2210 8th Street, Bldg 146, WPAFB, OH 45433, AIAA Associate Fellow.
[‡] Emeritus Professor, University of Dayton Research Institute, 300 College Park Avenue, Dayton, OH 45469, AIAA Fellow.
[§] Senior Research Engineer, University of Dayton Research Institute, 300 College Park Avenue, Dayton, OH 45469, AIAA member.

configuration. Phase 1 of the program dealt with development of this technology. Small high power density actuators and their supporting hardware were developed to drive the shape change. Various skin concepts capable of handling the large strain rates demanded by the changing geometry were considered. The skins must combine inplane flexibility with out of plane stiffness to maintain the aerodynamic shape. Phase II of the program is a wind tunnel demonstration in which contractors designs are showcased for down selection of a single concept to a phase III full scale morphing vehicle flight demonstration.

One concept to achieve this 200% wing area change is the Lockheed Martin folding wing aircraft shown in fig. 1, which illustrates the vehicle morphing from a cruise to high-speed dash configuration.
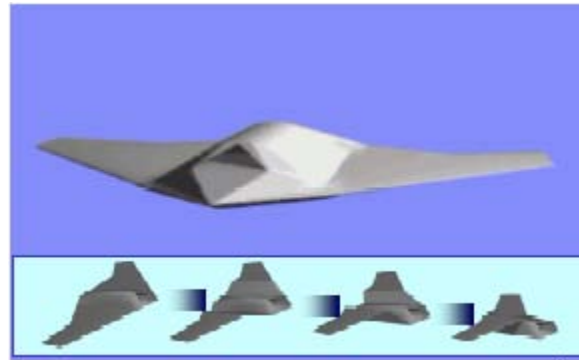

Figure 1: Lockheed Martin morphing vehicle[1]

Previous research[2] explains how the inclusion of a flexible wing fold hinge and sweeping of that hinge line can have the same positive affects as aeroelastic tailoring. However, Lockheed Martin takes this concept to the next level by folding the entire wing structure against the fuselage to radically reduce wing area as necessary for flight envelope expansion and improved performance. The change in wing area comes from two chord-wise wing folds, one at the wing root and the other at approximately 30% span. The wing folds are driven relative to each other, the inner wing folds approximately 130 degrees from the unfolded to the folded configuration while the outer wing remains in a flat condition. Flexible skins at the joints maintain the aerodynamic shape as the vehicle morphs. Shape control of the leading edge of the inner wing forces it to conform to the fuselage in the fully folded condition. Folding of the wing results in a wing area change on the order of 200%. This vast change in area enables the user to design unique mission profiles to take advantage of the characteristics of the flight vehicle.

This concept lends itself to unique application of aeroelastic considerations. Vibration modes will be impacted by the folding of the wing leading to changes in flutter speeds as the modes couple and uncouple throughout the fold range. The analysis presented herein shows how aeroelastic stability relates to the various fold positions of the wing during a standard mission. For this study a finite element model of the vehicle is used to establish the effects of changes in wing fold angle, wing hinge stiffness, and vehicle weight on flutter characteristics.

2. Problem Definition

A semi-span model (i.e. half fuselage and one wing) of the UAV is analyzed at various wing fold angles. Motion of the wing folding, morphing from the fully unfolded configuration to fully folded configuration, is expected to last thirty seconds, so quasi steady motion is analyzed by varying the wing fold angle by set increments. The following figure shows the model in the fully unfolded configuration, as well as multiple positions it will have during the morphing process. Note the fully folded configuration results in an inner wing fold angle of 130 degrees.
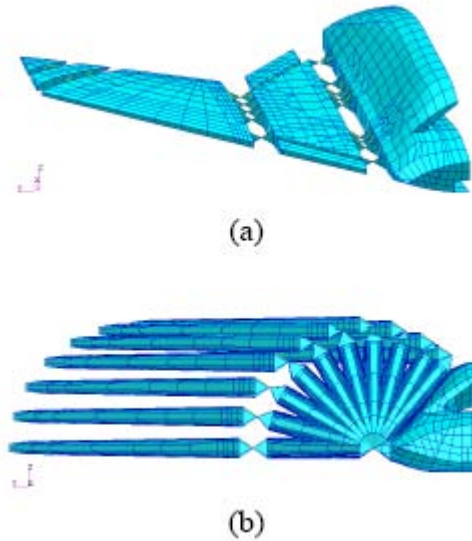
Figure 2: (a) Vehicle in fully extended configuration, and (b) various positions during morphing

The model contains three main sections: an inner wing, outer wing, and fuselage. The two wing sections are joined to each other and the fuselage by elastic elements with specified stiffness to represent the actuator mechanisms. The elastic elements allow rotation about the chord wise direction of the wing. As the wing folds these elements provide all of the stiffness in this direction. There are leading and trailing edge control surfaces on the inner wing in addition to an elevon on the outer wing. Composed of 5134 elements the 11,500 degree of freedom model is sized for the expected airloads. The aerodynamic models used for vibration and flutter analysis are NASTRAN flat-panel, doublet lattice models. Loads and displacements are transferred to the FEM through infinite plate splines. The aircraft is modeled in free flight with appropriate boundary conditions applied for symmetric and anti-symmetric analyses. Figure 3, a top down view, illustrates the structure of the finite element model.
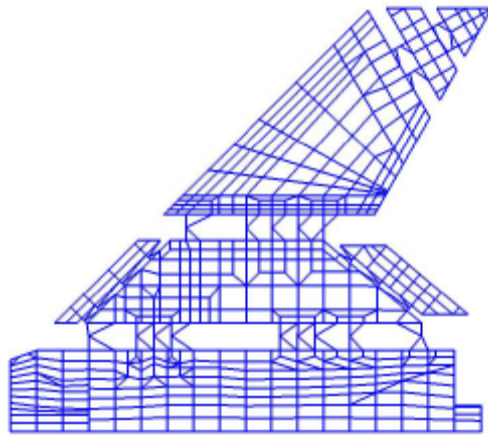

Figure 3: Finite element model illustration

Modal and flutter analyses are performed at several different mechanism stiffness', vehicle weight, and wing fold angle. The initial stiffness of the elastic hinge elements is roughly based on the stiffness of the leading edge control surface of a typical USAF fighter vehicle. Analyses are run at 10, 50, and 75 percent of those initial values. In actual operation a one order of magnitude reduction in stiffness may occur due to changes in properties of the advanced actuation materials implemented in the vehicle hinges. Once the desired wing fold angle is obtained, the stiffness of the mechanism returns to the original value.
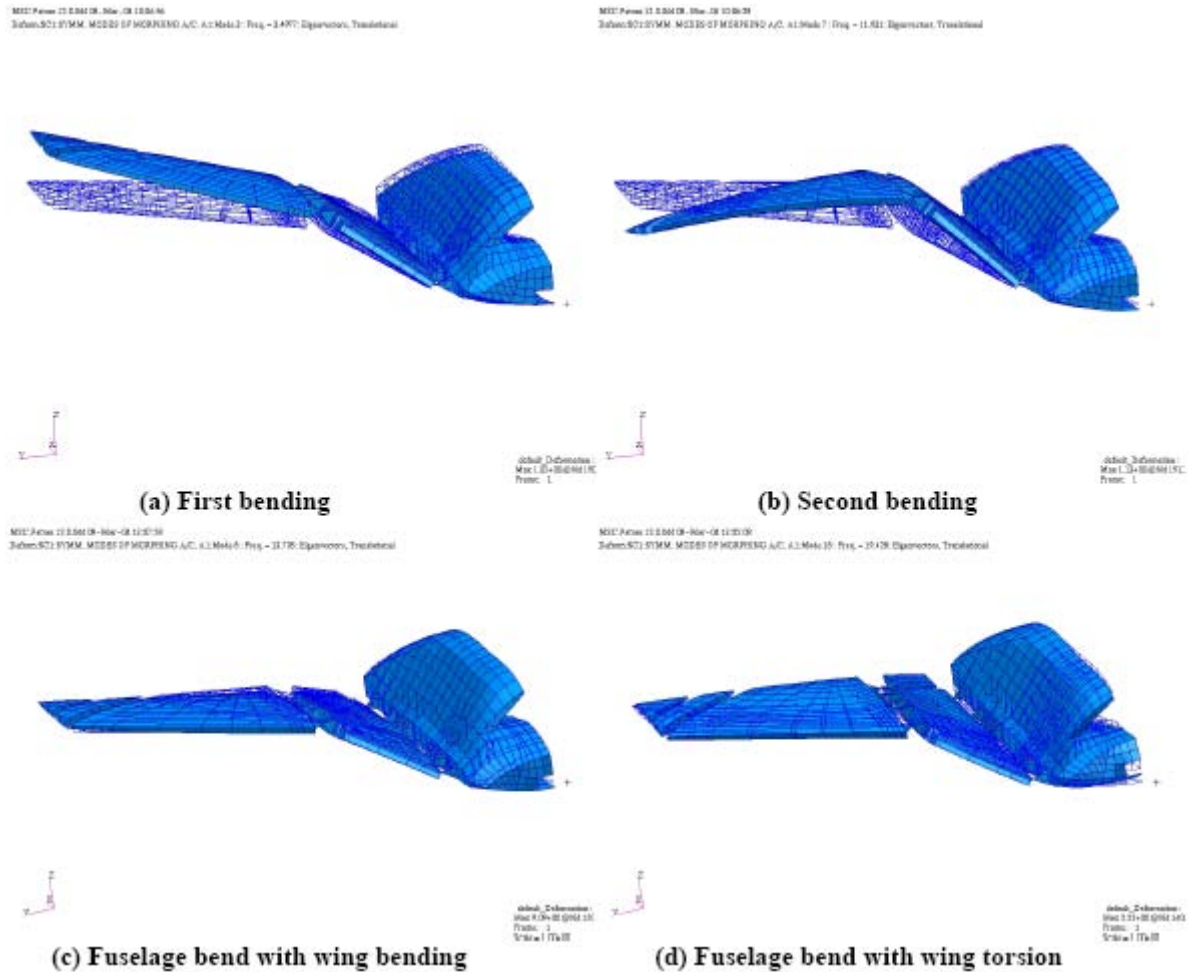
For this analysis wing fold angle varies at 15 degree increments from zero degrees, fully unfolded configuration, to 130 degrees, fully folded and latched configuration. Analysis is performed at two vehicle weights, take-off gross weight (TOGW) and empty weight configurations.

III. Results

The following paragraphs highlight the results of the modal and flutter analyses performed on the folding wing. Modal analysis data is presented first and is followed by the results of the flutter analysis.

A. Modal Analysis

For each fold angle, hinge stiffness, and weight configuration a modal analysis is run to collect resonant frequency data. Data from the first forty modes is collected; however, the majority of those modes are local modes, i.e. modes dominated by deformation of a single small panel. Mixed among the local modes are the global modes, modes where deformation occurs in a large part of the structure, that are of interest. Results are obtained from MSC NASTRAN using the Lanczos eigenextraction method and MSC PATRAN is used for visualization. The following figure shows the mode shape for the first six modes about a wing fold of 30 degrees.
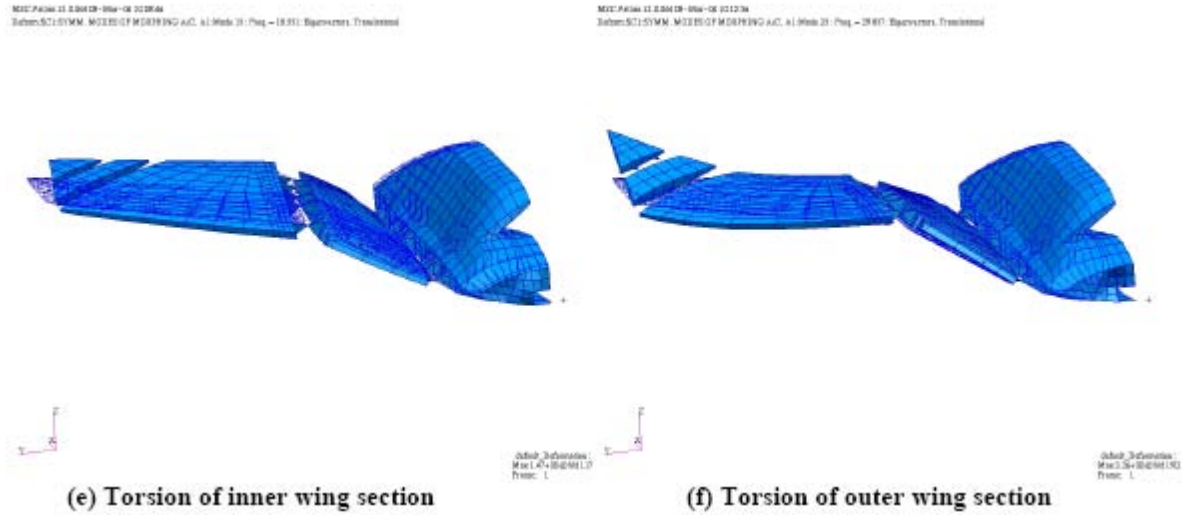
(a) First bending

(b) Second bending

(c) Fuselage bend with wing bending

(d) Fuselage bend with wing torsion

(e) Torsion of inner wing section   (f) Torsion of outer wing section

Figure 4: Modal analysis visualizations

The first and second bending modes are typical bending modes seen in structural analysis. The two fuselage bend modes are described as bending along the length of the fuselage in turn driving a wing response. In one case the fuselage bend leads to a wing torsion mode, in the other wing bending. Two torsion modes are seen, one is an inner wing torsion that, as the wing fold angle increases, drives a lateral sweeping motion in the outer wing. The second is torsion of the outer wing, which when excited generates little to no response in the inner wing. Visualizations such as figure 4 determined how individual modes changed as a function of variations in hinge stiffness, wing fold angle, and aircraft weight. For specified vehicle weight and hinge stiffness, plots were created to aid in data interpretation.

A plot of the data obtained for the baseline stiffness is shown in fig. 5. Data was taken assuming the aircraft to be at take-off gross weight (TOGW).
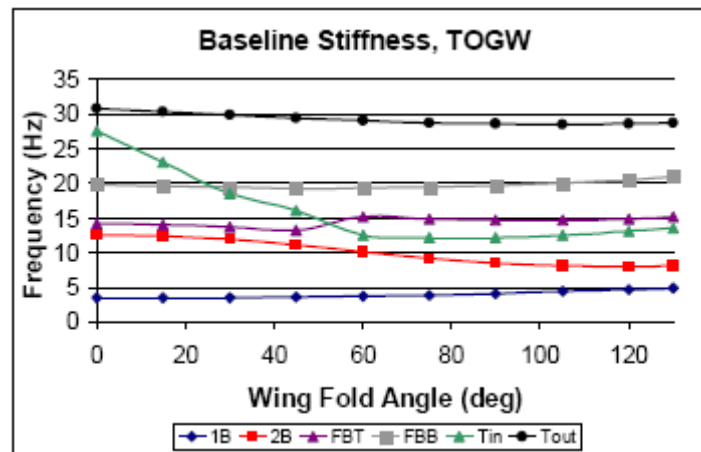

Figure 5: Plot of modal analysis results

1B represents the first bending mode, 2B the second bending mode, FBT is interpreted as fuselage bending driving wing torsion, FBB fuselage bending driving wind bending, Tin equates to torsion of the inner wing section and Tout torsion of the outer wing section. The x axis reports data at various fold angles between 0 and 130 degrees, data was taken in 15 degree increments. The first bending mode remains fairly constant in frequency throughout the range of fold angles and does not seem to couple with other modes. This seems to be true as well for the FBB and Tout modes. There is a drop, however, in the frequency of the second bend mode. It appears to couple with either the FBT or Tin mode between 45 and 60 degrees before once again separating. The FBT and Tin modes are items of interest due to the apparent mode switch that occurs between 45 and 60 degrees. There is remarkable

6

similarity between the two modes. At the zero degree fold angle there are subtle differences in the mode shapes that lend to this interpretation. The Tin mode is a pure torsion mode and the displacement of the wing tip is larger than the torsional displacement driven by the fuselage bending in the FBT mode. Likewise in the FBT mode the amount of bend in the fuselage is greater than that of the bending in the Tin mode. As the fold angle increases it is increasingly difficult to tell the modes apart simply based on the mode shape visualizations. In this case one turns to the displacement data and the knowledge gained from the zero degree configuration to discern the individual characteristics of the modes. Data shows this mode switch is structural as distinguishable characteristics of the modes can be found in the generated displacement data.

The symmetric and anti-symmetric modes are compared in fig. 6. As expected they mirror each other fairly well. The fuselage bend modes exist only the symmetric state and show are not shown on the plot.
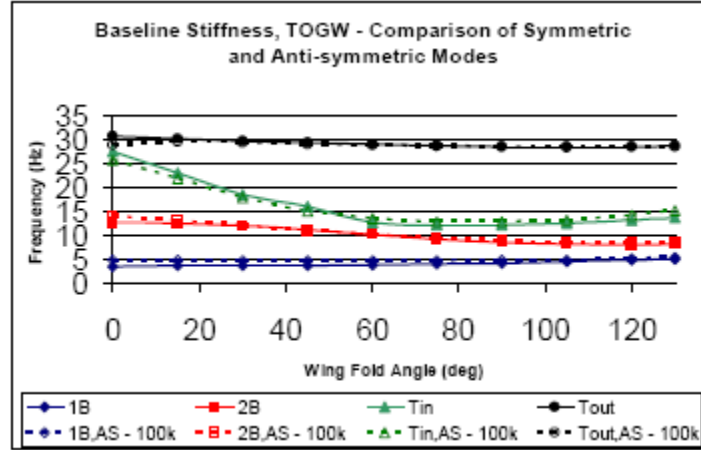

Figure 6: Symmetric and anti-symmetric mode comparison

Additional plots were created as hinge stiffness and weight varied. The ensuing plots show differences between the baseline case, initial stiffness and TOGW, for the sake of comparison and discussion. Figure 7 highlights differences between the baseline hinge stiffness and half hinge stiffness.
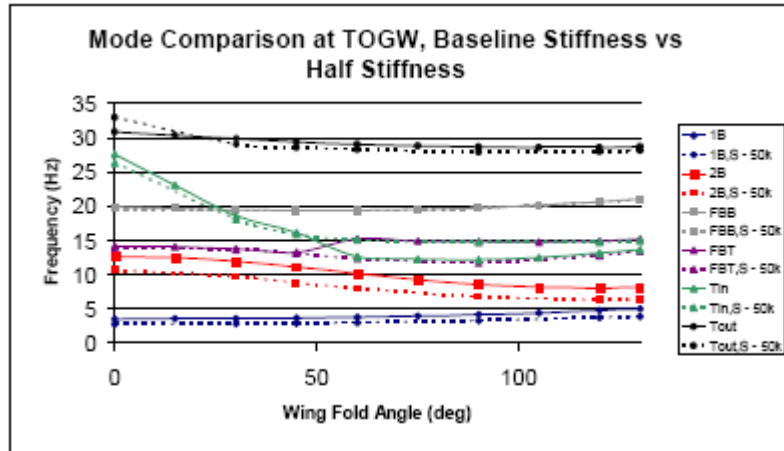

Figure 7: Mode comparison, baseline and half hinge stiffness

As expected, as a general trend, the frequencies of the modes from the half stiffness analysis are lower than those of the baseline stiffness. There are a couple of interesting observations. The Tout mode for the lower stiffness has a higher frequency at the 0 and 15 degree fold angle cases than the higher stiffness modes. Also, the mode switching seen in the higher stiffness case does not occur in the lower stiffness. As explained above it is felt that the mode switching was structural, not numerical. While this may not seem to be the case after reviewing the lower stiffness data, it is seen that the modal coupling that took place during the higher stiffness case is not as influential in

the lower stiffness study. It is very likely, then, that the switching would not take place in the lower stiffness case as the modal coupling is not as strong.

Not only was the stiffness reduced by 50% but there was also a case run where stiffness is reduced by an order of magnitude, shown in fig. 8.
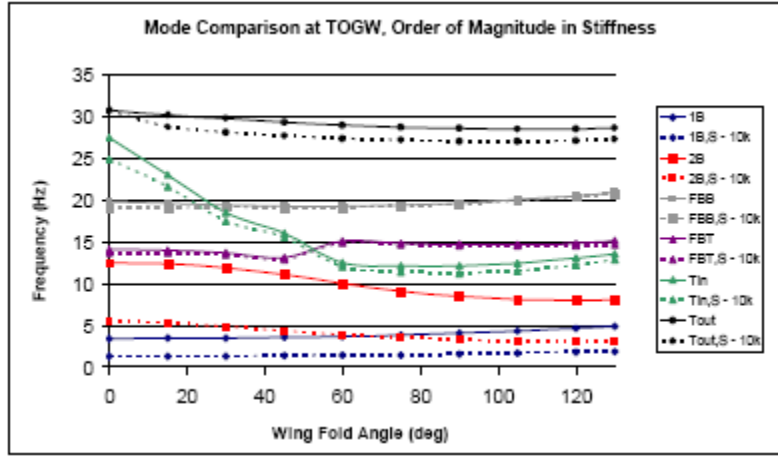

Figure 8: Mode comparison, order of magnitude difference in stiffness

The results are as expected, the less stiff wing has lower frequencies associated with the global modes. It is surprising that there is no mode switching in this case as there is clearly even less modal coupling than in the half-stiffness case.

A final series of analysis is made to determine the effect of vehicle weight on frequency. Results from the TOGW configuration were compared to an empty weight configuration for baseline hinge stiffness in fig. 9.
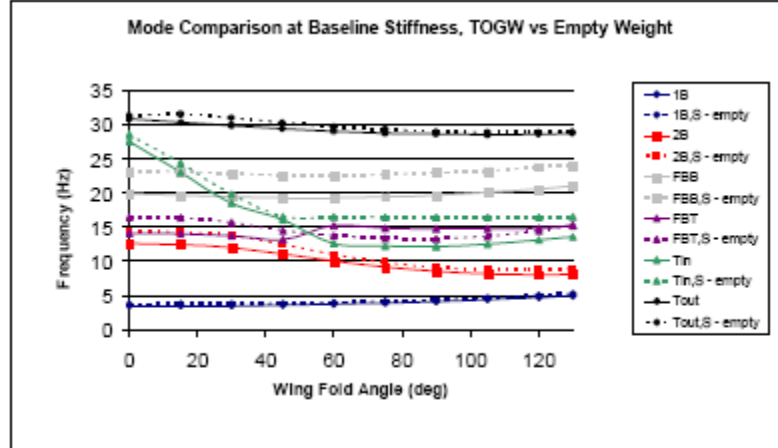

Figure 9: Mode comparison, TOGW vs empty weight

The results correspond to the general understanding that weight decreases the frequency of modes. As seen in the plot the frequencies of the empty vehicle are greater than those of the vehicle at TOGW. Once again it is interesting to note the mode switching between the Tin and FBT modes does not occur.

B. Flutter Analysis

Having completed a modal analysis attention is turned to the study of flutter phenomena associated with the folding wing. Using the PK method in MSC NASTRAN, tables of v-g and v-□ data are generated, and plotted for data comparison. Figure 10 is the plot for the baseline hinge stiffness, TOGW, zero degree fold angle case.
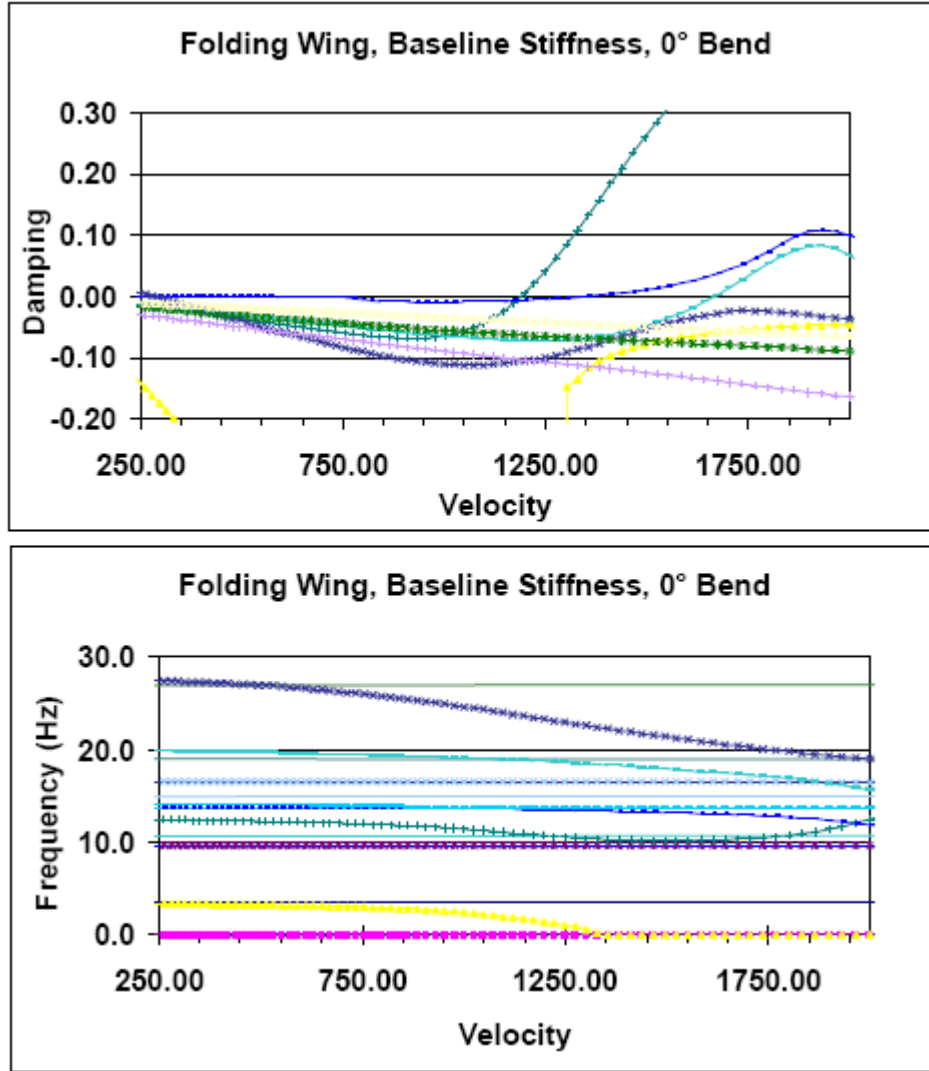
8

Figure 10: V-g, V-_ plots, baseline hinge stiffness, TOGW, 0 degree fold angle

The units of velocity are knots thus the plot indicates flutter speeds are out of the flight envelope for this case. Similar plots were generated at 30 degree fold angle intervals for each configuration. Flutter speeds identified from the V-g and V-ω plots are summarized in fig. 11.
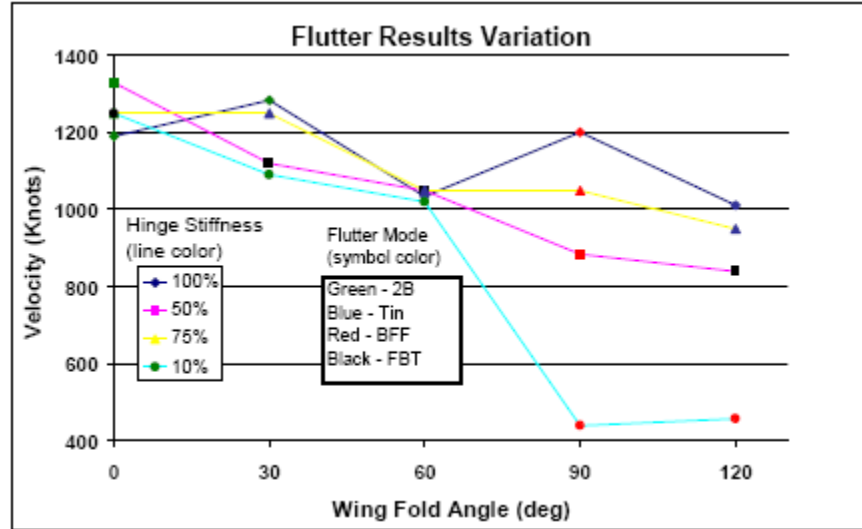
9

Figure 11: Flutter analysis results, TOGW

Figure 11 shows flutter results for four stiffness configurations all at TOGW. Following a line of constant color indicates a particular hinge stiffness while the marker color is indicative of the flutter mode. The dark blue line indicates flutter speeds in the baseline hinge stiffness configuration. As a function of fold angle and hinge stiffness flutter speed varies quite significantly and the flutter mode changes as well. Comparing this plot with the results generated in the modal analysis explains these results. The flutter mode in the zero degree wing fold angle is the second bend mode. Looking at the modal analysis results it is seen the second bend mode couples with the fuselage bend/wing torsion mode, likewise at the 30 degree wing fold angle case. However, at 60 degrees the flutter mode changes to Tin. This change occurs after the mode switching seen in the modal analysis. At 90 degrees the flutter mode changes again, this time to body freedom flutter which is the condition that occurs when the first bend mode couples with the short period mode. In the 90 and 120 degree wing fold angle cases, for a stiffness reduced by one order of magnitude, it is seen flutter speeds drop significantly. Other flutter mode switches can be traced in a similar fashion.

A final trade study was conducted for the empty weight configuration. The results are presented in tables 1 and 2.

Table 1: Flutter results for empty weight configuration, baseline stiffness

Wing Bend Angle	Flutter Velocity	Mode
0°	860	BFF
30°	840	BFF
60°	885	BFF
90°	1000	BFF
120°	930	FBT

Table 2: Flutter results for empty weight configuration, 10% stiffness

Wing Bend Angle	Flutter Velocity	Mode
0°	330	BFF
30°	300	BFF
60°	315	BFF
90°	350	BFF
120°	400	BFF

As seen from table 2 the flutter velocities are much lower, all within the flight envelope, and all display body freedom flutter as the flutter mode.

Divergence analyses show divergence speeds are greater than flutter speeds for all cases. A divergence analysis is run to verify divergence speeds derived from the V-g and V-f diagrams are accurate.

IV. Conclusions

The data shows strong interrelationships between fold angle, hinge stiffness, and weight of the Lockheed morphing vehicle. The modal analysis data shows bending modes are greatly impacted by changing the hinge stiffness. As the hinge stiffness increases above the structural stiffness the unfolded configuration bending modes become those demonstrated by more traditional wings. As wing fold angle is increased the bending modes are primarily functions of the structural stiffness for the higher spring stiffness. Torsion modes are likewise impacted by the changing hinge stiffness and, as the frequencies of the modes increase with increasing stiffness, the modes begin to interact. This modal coalescence is tied to results seen in the flutter analysis. The mode switching that takes place leads the flutter mode switching to inner wing torsion or body freedom flutter. The weight of the vehicle also plays a significant role in the flutter mode. Table 2 shows body freedom flutter may be a concern as the vehicle approaches its empty weight. Body freedom flutter is the flutter mode at 90 degrees for all configurations. However, at higher stiffnesses the flutter mode changes back to inner wing torsion as wing fold angle increases past 90 degrees. At empty weight body freedom flutter is the only flutter mode seen in the analysis. As most of the results show there is little concern for this particular vehicle, however, care must be taken when it is known the actuation system is providing little stiffness resistance. Actuation systems which are not of the traditional hydraulic kind, but invoke thermal or other such similar properties may be of concern during vehicle configuration transition.

References

1. Love, H.H., Zink, P.S., Stroud, R.L., Bye, D.R., Chase, C., "Impact of Actuation Concepts on Morphing Aircraft Structures, *45th AIAA/ASME/ASCE /AHS/ASC Structures, Structural Dynamics & Materials Conference* 19 - 22 April 2004, Palm Springs, California.

2. Pitt, D.M., "Static and Dynamic Aeroelastic Analysis of Structural Wing Fold Hinges That are Employed as an Aeroelastic Tailoring Tool", *45th AIAA/ASME/ASCE /AHS/ASC Structures, Structural Dynamics & Materials Conference* 19 - 22 April 2004, Palm Springs, California

Simulation Tool for Analyzing Complex Shape-Changing Mechanisms in Aircraft

Jason C. Bowman,[**] Gregory W. Reich,[††] and Brian Sanders[‡‡]
Air Vehicles Directorate, Air Force Research Laboratory, WPAFB, OH 45433

and

Geoffrey J. Frank[§§]
University of Dayton Research Institute, Dayton, OH 45469

This paper describes the development of a simulation tool to study the time domain, in-flight behavior of aircraft morphing mechanisms. With appropriate modifications for particular problems, however, the approach is general enough to handle any load-bearing structure with time-varying shape or position. The motivation and requirement for such a tool is discussed, and the framework of the tool is presented. The development progression, current state-of-the-art, and planned development of the tool are illustrated through application to a folding wing vehicle.

Nomenclature

F_M	=	total modal load vector
$\mathbf{q}$	=	vector of ADAMS degrees of freedom
t	=	time
s	=	modal force weighting function
g	=	individual modal force weights
F	=	constant modal load
Φ	=	matrix of Craig-Bampton component modes
q_∞	=	freestream dynamic pressure
α	=	angle of attack
δ	=	vector of control surface deflections

I.   Introduction

The progression of morphing technology over the past decade has highlighted the use of new materials, actuators, and mechanisms to achieve large aircraft shape changes. Several years ago, a morphing program was initiated to bring these technologies together onto flight-traceable structures to be wind tunnel tested. An effort at the Air Force Research Laboratory was initiated in parallel to begin to answer how these technologies behave and interact on a realistic aircraft structure.

The morphing concepts developed in the morphing program are shown in Figure 1. For the one degree-of-freedom Lockheed folding wing concept, the morphing actuators are in the wing bending load path, the skins on the hinges must be seamless, and there are aeroelastic stability (flutter) considerations over a certain range of fold angles. For the NextGen concept, actuator placement and the number of total actuators required, force fighting between actuators and binding of the mechanism, and mechanism instabilities such as overcenter or snap-through are major challenges. For a two or more degree-of-freedom mechanism such as the NextGen concept, there are an infinite number of paths between two wing positions. Some paths may produce unstable vehicle configurations yet no

---

binding or force fighting. Other paths that produce stable vehicle configurations may be infeasible due to force fighting between actuators. For both, the extra degrees of freedom afforded by morphing makes identifying both adverse and favorable (e.g. air load actuation) interactions between mechanism, aerodynamics, actuator control systems, and vehicle flight control systems even more important.
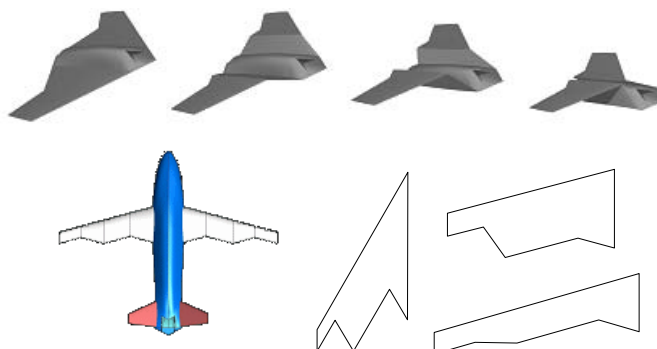

Figure 1: Lockheed and NextGen Aeronautics Morphing Concepts

Without morphing, for example, a traditional flutter analysis can be completed without simulation. To compute flutter speeds, it is sufficient to know the stiffness of the structure and some aerodynamic properties. The (time) history of how the structure got into a flutter is often irrelevant, just that it flutters at a certain speed. However, for morphing wings, the morphing may be fast enough to transition through flutter regions that the flutter dynamics do not have time to fully develop. Simulating a situation such as this in a time-dependent manner allows a designer to see if the structural dynamics are tolerable and that the control systems can adequately compensate.

Another situation that lends itself well to a time-dependent analysis is the reaction of the vehicle to various maneuver commands. Various loads on the mechanism throughout the maneuver may prevent the mechanism from achieving certain positions. Deformation in the structure may cause unpredicted force fighting or binding. Furthermore, it is entirely conceivable that specific load cases in a specific order occurring at a certain rate may allow the mechanism to go into positions it would not normally be capable of and end up in a locked state.

Simply put, quasi steady-state analysis at multiple morphing states may not be adequate to understand the system behavior. And unsteady effects in the computation of loads depends on the time and length scales at which the morphing, vehicle maneuvers, and transient structural dynamics occur. The dynamic aeroelastic behavior of the vehicle may not be a critical aspect to capture in the simulation, but the unsteadiness in wakes and boundary conditions may be important if the morphing action is fast enough. A comparison of responses incorporating different aerodynamic effects can highlight the important unsteadiness as well as the terms that have minimal effect on the overall system behavior.

Structurally, the interaction between flexible bodies and kinematic mechanisms is extremely important for morphing performance, especially for morphing systems that accomplish shape change through in-plane deformation of the wing. Aeroelastic wing deformation can cause binding and locking of a mechanism, which can be analyzed in a simulation environment. Incorporation of the aerodynamics into a multibody analysis tool allows the designer to compute complex aerodynamic loads that are highly dependent on the position of the mechanism. The incorporation of actuator dynamics also increases the accuracy of the structural response by inclusion of the stiffness and damping inherent in the actuation system.

As an example of some of these issues, a morphing wing was tested at the Air Force Research Laboratory's Multiaxis Test Rig facility in 2005. Several path-dependent force fighting issues were identified and resolved through a combination of mechanism path changes and actuator control algorithm development. Had a computer tool been available that was capable of modeling the plant correctly, it may have been possible to identify problems and solutions in the design and development phase. Furthermore, although this laboratory testing was specifically risk reduction for a wind tunnel test, a tool, if available, would allow the designer to also validate the vehicle

stability as part of the test. While this could have been validated separately, having a simulation tool available makes it possible to conduct simultaneous design and refinement.

What is the current state of the art in the analysis and simulation flexible multibody dynamics with aerodynamic loading? Clearly, there are a number of codes that do individual aspects of this problem very well. Multibody dynamics codes such as ADAMS and DYMORE can be used to model rigid or flexible bodies under various loading conditions, but lack the fidelity of aerodynamic analysis required for complex distributed time-varying loads. The current generation of structural design tools used for aeroelastic loads analysis (such as NASTRAN, ASTROS, etc) was developed for static or dynamic analysis of time-invariant structures, and therefore by definition cannot be used to analyze morphing structures in a time-varying manner. These tools can also analyze the structural response of an aircraft in simple maneuvers, but do not include any control capability beyond perhaps a trim optimization procedure to find a trim point for a given maneuver.

Clearly, then, there is a need for a tool that allows the engineer to simulate the performance of a morphing vehicle in a time-dependent manner during a morphing maneuver. At a minimum, the tool should incorporate aerodynamics with time-varying, flexible wakes, flexible and rigid-body motion of the structure, and a flight control system capable of creating morphing maneuvers and providing vehicle stability during flight.

The remainder of the paper is divided into two parts: the first part describes in more detail the current capabilities of an interaction between NASTRAN and ADAMS. The second part describes the development and capabilities of a new tool based on ADAMS, NASTRAN, vortex-lattice aerodynamics , and Simulink that is an improvement on the first, and enables a designer to analyze and simulate a time-varying, flexible, multibody, flying morphing vehicle. Both parts will contain examples that highlight the capabilities and limitations of each. A time-scale analysis, while beyond the scope of the present paper, is also in the works to understand the interaction between aerodynamics, vehicle and mechanism kinematics, and structural flexibility at different time scales.

II. Current Capabilities

NASTRAN at its core is a finite-element tool, but as mentioned in the Introduction, it has the capability for basic aeroelastic trim analysis through an integrated aerodynamic tool. ADAMS is, at its core, a multibody dynamics simulation tool that has been used extensively in the automotive industry and increasingly in aerospace to simulate complex mechanical systems.

ADAMS has the ability to incorporate both rigid and flexible bodies in a simulation. Flexible bodies can be generated from rigid structures created within ADAMS or from modal representations from external sources such as NASTRAN. The particular modal representation used is a Craig-Bampton component mode synthesis[1] process. The full importance will become apparent shortly, but rather than represent a full vehicle modally, a component mode synthesis allows modes to be computed for individual pieces and then later summed. Distributed loads for flexible bodies can also be imported into ADAMS via a modal load definition, which allows for aerodynamic loads to be incorporated in certain limited cases. Additionally, loads may also be incorporated directly through functions written by the user.

Consider the first approach for applying loads. From NASTRAN, the vehicle finite element model is imported into ADAMS. The baseline aerodynamic loads at a given trim state can also be imported, along with load sensitivities due to angle of attack or control surface deflections. Then, in ADAMS, the total aerodynamic loads could be written as

$$F = q_\infty \left[F_{baseline} + \alpha \frac{\partial F}{\partial \alpha} + \sum \delta_i \frac{\partial F}{\partial \delta_i} + \omega \frac{\partial F}{\partial \omega} \right] \qquad (1)$$

where α is a known function of angle of attack, δ is a vector of known control surface deflections, and ω is the rigid body angular velocity. Until recently, however, the other parameters inside the brackets of Eq. (1) had to remain constant due to a limitation in ADAMS. A control system can also be incorporated into a simulation in order to command the trim parameters. Note that compressibility effects are not considered here, but could also be added to

Eq. (1). As long as the vehicle does not violate any of the basic assumptions that result from the importation of the aerodynamic loads, then the loads applied to the vehicle should be accurate (at least to the level of accuracy of the original loads computation).

Simulations of this type have been demonstrated by McConville et al[3]. They simulated a vehicle performing a "lob" maneuver, which is a climb and simultaneous stores release. The vehicle was modeled as a single flexible body imported from NASTRAN, while the store was a separate aerodynamic body. Baseline aerodynamic data for a given trim condition was imported into ADAMS. Aerodynamic load sensitivities with respect to control surface deflections were also imported. The maneuver was then created in ADAMS by creating functions of control deflections, velocity, and other vehicle state information to control the aircraft trajectory.
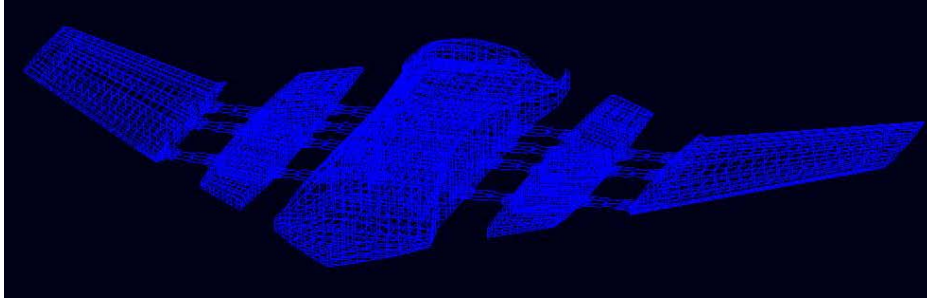

Figure 2: Free-flying model as a single flexible body.

As another example, consider the vehicle shown in Figure 1. It is a symmetric, free-flying version of a Lockheed-Martin morphing wind tunnel model[4] in the unfolded configuration. The finite element model has been imported from NASTRAN into ADAMS as a single flexible body. Steady aerodynamic loads are computed for the basic vehicle, and sensitivities are included for control surface deflections and angle of attack. These loads are imported into ADAMS as modal loads, which mean that the physical loads and load increments have been pre-multiplied by the Craig-Bampton component modes related to the flexible body. Vehicle simulation is then achieved by computing aerodynamic loads from the combination of trim parameters and dynamic pressure, which are pre-defined.

Now consider the case of a morphing vehicle, one in which the basic vehicle geometry can change with time. The ability to represent forces as functions of geometry in Eq. (1) now becomes important. However, computing loads in the form of Eq. (1) can be prohibitively expensive. First consider the non-morphing, rigid body case. In the usual representation outside of ADAMS, the basic aerodynamic load consists of approximately fifteen parameters, give or take a few depending on the representation, that are generally functions of angle-of-attack, sideslip angle, Mach number, and Reynolds number. These are the basic forces and moments (six) and incremental forces and moments due to rigid body rotation rates (nine). Added to these loads are the loads due to control effectors, which are generally functions of the same parameters. Depending on the situation, it is sometimes possible to reduce the dimensionality of the problem by ignoring Reynolds number effects, sideslip on effectors, and angle-of-attack on rate derivatives for example. With morphing added but still considering a rigid body, the dimensionality of the problem grows by twice the number of morphing degrees of freedom – one factor for the morphing position and the other factor for the morphing rates (the rate influences the boundary condition). Adding flexibility to the problem makes the representation of loads in the form of Eq. (1) intractable because now the incremental effect of all of the modes plus the local velocities induced by local deformation now have to be considered as well.

III.   Integrated Aeroelastic Multi-body Morphing Simulation

So what is different with an integrated simulation tool? The big difference comes in the computation and application of the aerodynamics loads. Rather than pre-computing a set of steady loads and sensitivities as table lookups or writing these as functions, the aerodynamic loads are computed based on the exact geometry and boundary conditions at each time step for the current morphing shape. The spline or interpolation between the aerodynamic grid and the structural model is also re-computed at each time step. The quality of the loads is only dependent on the aerodynamic tool used. For quick analysis, one might choose a vortex lattice approach. For a more detailed, focused analysis, one might choose an Euler code or CFD.

The tool that has been developed is called IAMMS: Integrated Aeroelastic Multi-body Morphing Simulation. The tool is based around the ADAMS multibody dynamics code, which is utilized to perform time integration of the equations of motion for the multi-body representation of the morphing aircraft. Loading is computed at each time

step by an AFRL-developed code, which uses a vortex lattice method for computation of the aerodynamic loads and splining techniques to interpolate the aerodynamic forces onto the structure. An automatic flight control system is included using a Matlab/SIMULINK-based multi-loop feedback control system developed by AFRL. The inner control loop uses dynamic inversion, while the outer loop includes standard Proportional-Integral-Derivative (PID) controllers.

For IAMMS, models are typically created in ADAMS via the flexible body interface with NASTRAN. Each component must be created separately so that ADAMS can treat them as separate parts. If the entire vehicle is read in as a single flexible body, then no rigid-body motion can occur between components that are included in the flexible body. Just as important is that the modal representation needs to be only computed for each component once. The Craig-Bampton component mode synthesis will take the component modes and sum them properly. The component modes plus the combination of morphing position and boundary conditions at the joints connecting the components uniquely determines the full vehicle modes. Consider the vehicle in Figure 3. It is slightly different version of the same free-flying MAS wind tunnel model from Lockheed. In Figure 3, each of the major components, the outer wings, inner wings, and the fuselage, are all shown in different colors to indicate that they are separate bodies, rather than all in the same color as in Figure 1 where the entire vehicle was represented by a single flexible body.
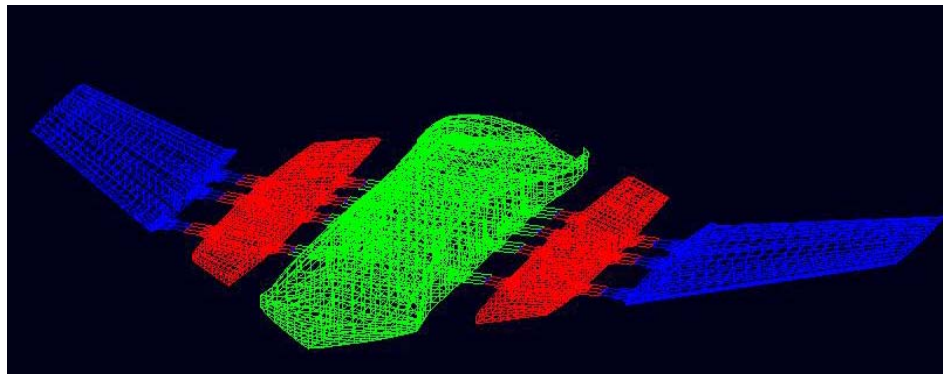

Figure 3: Free-flying model as separate bodies.

The flexible bodies are connected in ADAMS by joints. The complex drive and actuation system used on the wind tunnel model has been simplified for this simulation, while retaining the key effect of joint flexibility. Figure 4 shows a close-up of one of the joints along the outer right hingeline. The joint consists of three small disks. Two of the disks are rigidly attached to the flexible bodies, one on each side (indicated by the lock icons). The third disk is attached to each of the other two with revolute joints. One joint includes a torsional spring (the yellow arrow icon) to model the flexibility of the actuation system, and the motion of the other joint is commanded as the wing fold position command produced by the control system (the white arrow icon).
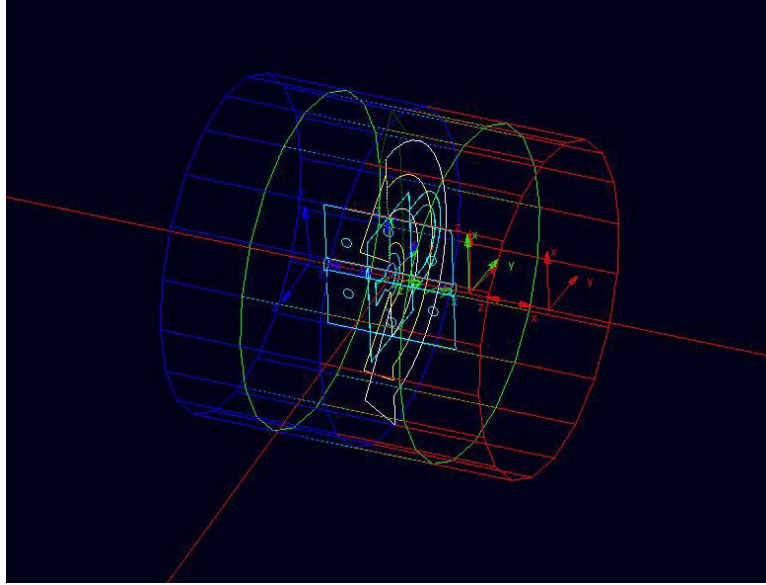
Figure 4: Close-up of a joint.

Note that there are multiple hinge attachment locations on each fold line. For rigid bodies, these represent redundant constraints. For flexible bodies, multiple attachments are permissible because the flexibility in the bodies allows for numerical noise and misalignment in the joints.

Aerodynamic loads are created on this model via an in-house vortex lattice code. The aerodynamic panel model, such as the unfolded configuration shown in Figure 5, is created at each time step based on the current position of the wing components. A splining process, very similar to the methods implemented in NASTRAN[6] and ASTROS[7], is utilized to determine the shape of the panel model based on the motion of the joints and the flexibility of the structure. The current vehicle state (position, orientation, rigid body rates, and local velocities due to local deformation) is also fed to the aerodynamic analysis, which returns loads at the center of each aero panel. The splining routine then transfers the aerodynamic panel loads to a set of structural load points on each body.
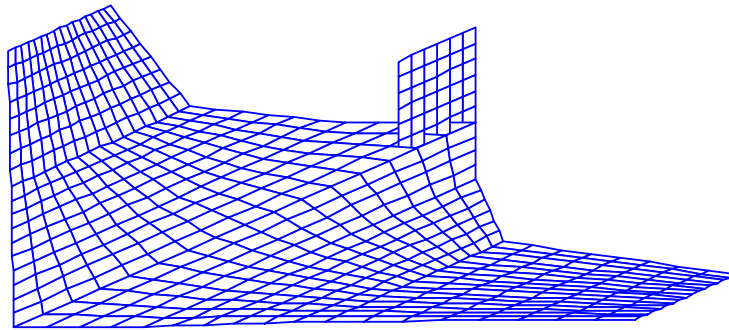

Figure 5: Aerodynamic panel model of the folding wing vehicle.

Note that the panel model in Figure 5 includes a horizontal tail that does not appear on the wind tunnel model. This fictional surface, as well as a fictional rudder, has been added in order to control the lateral/directional behavior of the vehicle that would normally be controlled with thrust vectoring. Additionally, fictional trailing-edge control surfaces have been added to the outer wings to provide longitudinal control. The wind tunnel model was not designed with any of these surfaces, and they are not precise representations of the control surfaces that a vehicle of this sort would actually use. They are simply convenient surfaces to have for stability and control of the free-flying vehicle. In addition to the fictional control surfaces, an applied thrust vector has been added as an additional control

parameter. Since the in-house vortex lattice code is in an alpha state and drag is not being computed, excess thrust is computed in the control routine as a commanded thrust from an engine model minus a drag estimate and is input to the vehicle as a control input force.

To control the vehicle, a flight control system in Matlab/SIMULINK was linked to the ADAMS model. To provide this control system with the correct plant information, a number of measures and state variables were created in the ADAMS model. These measures included the vehicle state (position, orientation, and rates) as well as the current morphing configuration. ADAMS provides for an interface to SIMULINK via a "control system export" which creates a model for insertion into the control system diagram. This plant model, when called in SIMULINK, spawns an ADAMS/Solver process which loads the model and simulates the plant dynamics based on the control system inputs (thrust, control surface deflections, and morphing parameters).

The control system itself is a multi-loop vehicle stability and control scheme. The inner loop, which controls vehicle angular rates (pitch, roll, and yaw) is based on a dynamic inversion process[8]. This takes a model of the plant (in this case a stability and control model, interpolated from a suite of pre-determined morphing parameter models), inverts it, and then assigns closed-loop poles to meet some performance objective. The outer loop controls heading, altitude, speed, and other performance objectives directly through classical PID controls.

The simulation process, represented in Figure 5, actually is driven by the control system in SIMULINK. The performance objectives, including morphing profile, are set here, along with the total simulation time, control system time step, and plant/feedback communication interval. On initialization, the simulation spawns the ADAMS/Solver process, and the two processes run side-by-side. They are separate processes, can have separate integration time steps, and only swap input/output data at specific time intervals (the communication interval). This is called a "co-simulation", and while it is not the only method to integrate the ADAMS and SIMULINK processes, it is a very convenient and straightforward method to do so.

The ADAMS simulation itself is run based on settings in ADAMS/Solver. These settings control the type of numerical integration scheme used, the accuracy of the predictor/corrector and convergence of the various iterative steps in the process, etc. The solver also internally controls the step size for integration, as this is independent of the step size used by SIMULINK. In each time step, the solver collects all of the loads applied to the system. In order to compute the aerodynamic loads, the subroutine at the heart of IAMMS first queries the model for the vehicle state from the previous time step. This information (position, velocity, orientation, morphing positions and velocities with respect to the center of mass (CG), deformation of the flexible bodies, etc) is used to compute the aerodynamic panel model for the current time step. The aerodynamic code then computes the aerodynamic forces on the vehicle, which are splined back to the structural components.

There are a few limitations to this simulation process. First, in the area of structural representation, the joint model does not accurately represent the actuation drive system for the wing fold. A simple torsional spring stiffness and damping is used to represent the potential flexibility in this system, but nothing is done to represent limitations in actuation force or power output. Second, in the area of aerodynamic force computation, a vortex lattice representation has its own limitations. It is based on potential theory and cannot estimate friction drag forces without modification, which is currently being considered. Being in an alpha state, induced drag is also not being computed directly. To overcome these drag deficiencies, a estimated drag polar is used in the control system in conjunction with the engine model to estimate the excess thrust that is applied to the aircraft, but this is applied to the vehicle center of gravity. Drag forces would normally be distributed. This may be important for an in-plane sweep motion where binding may be an issue, but it was not considered a important factor for a out-of-plane wing
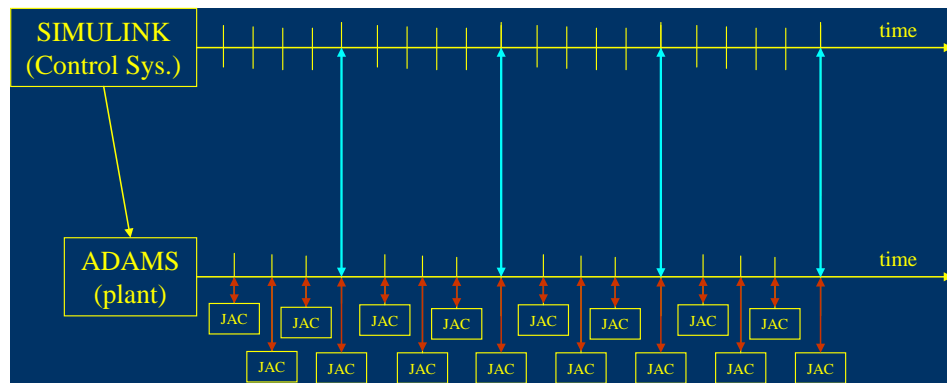

Figure 5: Co-simulation procedure for IAMMS.

18

fold mechanism. Finally, a vortex lattice representation is a lifting surface model. While able to model camber, which was not modeled in this analysis for simplicity, thickness effects can not be modeled. The thickness effect is negligible at small fold angles. However, at fold angles approaching and above 90 degrees, the interference between the inner and outer wings and the inner wings and fuselage due to thickness become quite important. More accurate aerodynamic codes need to be utilized to properly characterize the loads in these configurations. That being said, a CFD comparison with wind tunnel loads at high fold angles was even off. For the purposes of this simulation, the fold angles are never commanded beyond 60 degrees or so, which allows accurate load estimation with a lift surface representation.

IV. Results

To demonstrate the utility of the IAMMS process, simple simulations of the model shown in Figure 2 have been computed. A level-flight scenario, a climb to altitude, a heading change, and a morph while maintaining altitude all demonstrate the capabilities of the simulation. The simulation results are best observed as time-doamin movies, which obviously cannot be included in printed paper. However, it is possible to show some of the outputs and states as related to the commands, which are presented below.

Figure 6 shows the simulation results for level flight (commanded 10,000 ft altitude, constant speed). The simulation starts just slightly above 10,000 ft, but not quite at equilibrium. During the first two seconds, the vehicle drops about 9 feet, and the control surfaces and angle of attack adjust in order to recover the altitude loss. After about 2 seconds, the model is in equilibrium and regaining altitude. From this time on, the vehicle maintains heading, speed, and altitude. In Figure 6 a number of different parameters are plotted. In the upper left of Figure 6, a snapshot of the vehicle is shown during the animation of the simulation results. The white line is a trace of the vehicle center of gravity (CG) during the simulation. At the upper right, the vehicle altitude is shown. The altitude command is 10,000 ft, and while the initial condition is just under 10,008 ft, the correct altitude is quickly recovered with overshoot of only about 1 ft. Other parameters shown in the figure include the angle of attack, control surface deflection, vehicle pitch rate about the CG, and the vehicle's speed, which increases from the commanded initial 650 ft/sec as the vehicle descends, and then recovers to the commanded rate after a few seconds.

A more interesting simulation is a simple morphing simulation. The same simulation as shown in Figure 6 is repeated, except that at 2 seconds, a wing fold command of 4 deg/sec is initiated. These results appear in Figure 7. In this figure, the model is shown at an intermediate time step of 9.94 sec, where the wings are folded at approximately 32 deg. Also shown in the figure are angle of attack, control surface deflection, speed, and wing fold angle, all as functions of time. What is interesting about this figure is the behavior of the model after the fold initiates at 2.0 sec. At 2.5 sec, a rather large spike in angle of attack and control surface deflections are seen. The source of this spike is not completely understood, but appears to be an artifact of the control system reacting to the startup acceleration of the wing fold. Because of this behavior, the altitude increases back up to 10,006 ft, which may seem like a large increase in the figure, but in reality is only a 0.06% increase in altitude.

At about the 4.0 sec point, the vehicle has regained its commanded speed, and the control system now attempts to bring the model back to the commanded altitude while continuing the folding action. What is interesting here is
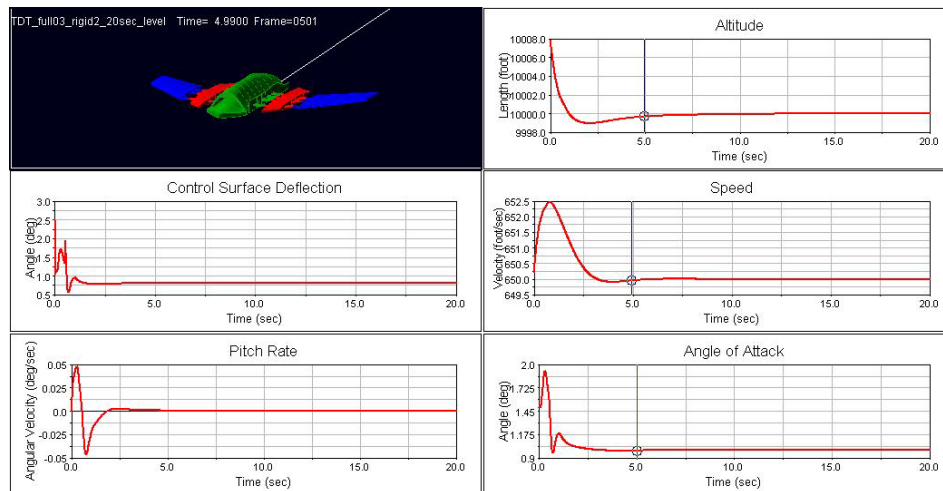

Figure 6: Results from a simple level-flight simulation.

that the control surface deflections are decreasing, while the angle of attack increases. The control surfaces are not needed as they provide a nose-down pitching moment that is undesirable – the model is in trim at this point. The angle of attack increases in order to offset the reduction in lifting area of the wings caused by the folding action. This is more clearly seen in Figure 8, which shows the angle of attack plotted against the wing fold angle. After the angle of attack transients clear out, around the 5.0 sec mark, the angle of attack is nearly linear with respect to wing fold angle. Another interesting phenomenon in Figure 7 is the small blips observed in control surface deflection and angle of attack between 15.0 and 18.0 sec. These small spikes are due to the mechanism binding up. The alignment of the different parts in the model is not numerically perfect – there are small numerical misalignments that cause the parts to move imperfectly with respect to one another.

Other simulations completed with this same model have similar results. Figure 9 shows a climb from 10,000 to 11,000 ft. Figure 10 demonstrates a 5 degree heading change at constant altitude and constant zero wing fold angle. These simulations demonstrate the ability of the flight control system to control the vehicle during flight.

V.   Conclusion

A tool for free-flying simulation of a morphing vehicle has been developed. The tool combines a multibody dynamic simulation package with an aerodynamic code for load computation and a Matlab-based flight control
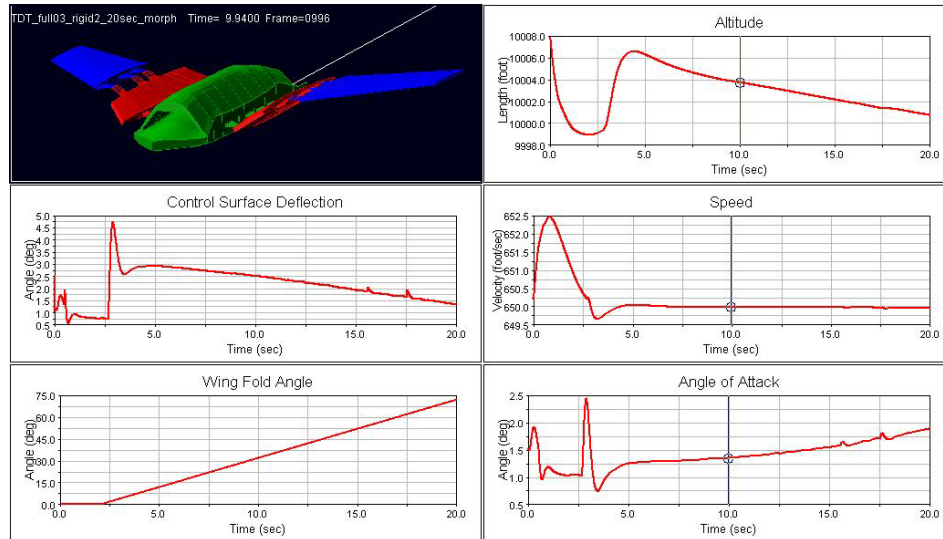

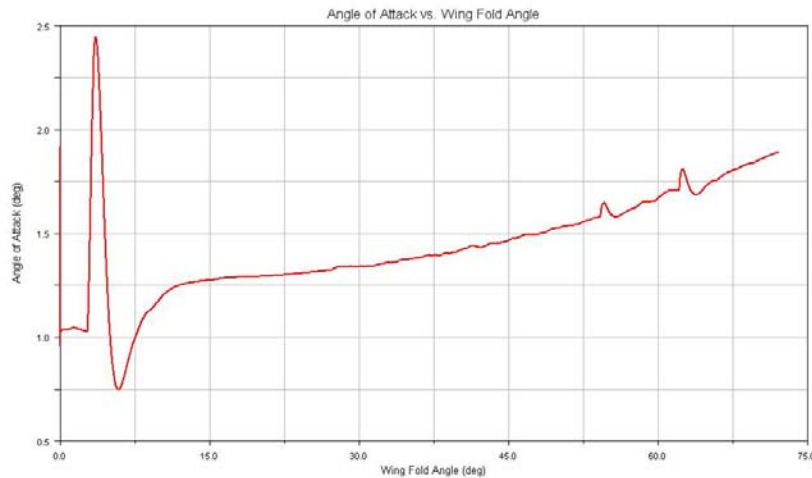**Figure 7: Result from level-flight morphing simulation.**

Figure 8: Angle of attack plotted against fold angle for the morphing simulation.
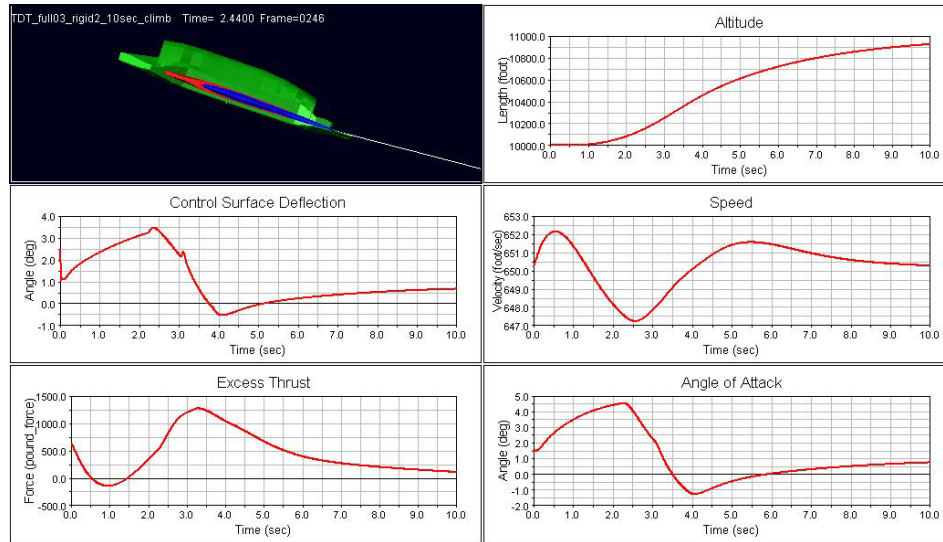
20

Figure 9: Results of a simple climb maneuver.

system. Key features of the tool include the ability to model both non-linear large rigid-body motions and linear
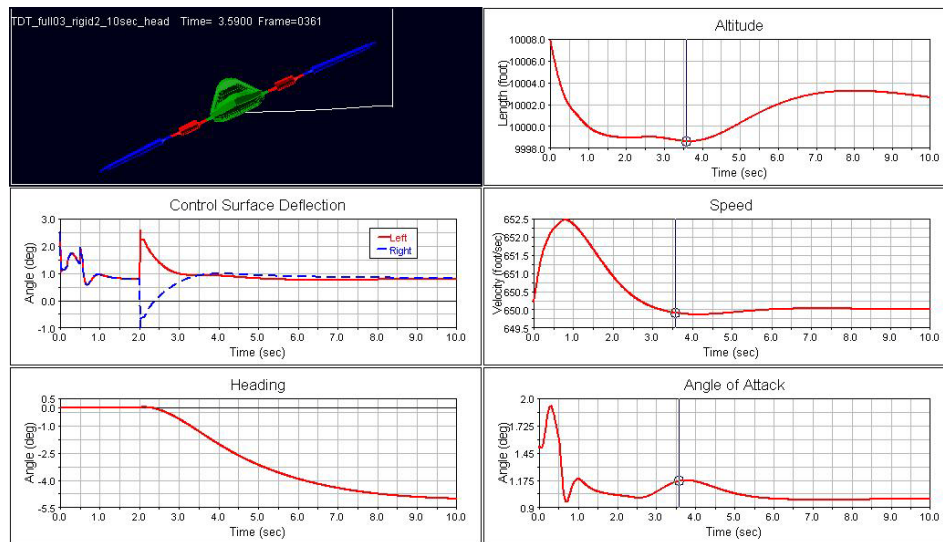

Figure 10: Results of a simple heading change.

flexible-body deformations, and the integration of an aerodynamics package that allows for complete aerodynamic loads to be computed based on the current configuration at each integration step. The tool is used to simulate the flight of a simple folding wing vehicle concept, which demonstrates several performance phenomena of this type of vehicle.

References

[1]Craig, R. R. and Bampton, M. C. C., "Coupling of Substructures for Dynamic Analyses," *AIAA Journal*, Vol. 6, No. 7, 1968, pp. 1313-1319.

[2]"Using the State-Dependent Modal Force (MFORCE)," AFL-005, ver. 2005 r2, MSC.Software, Santa Ana, CA.

[3]McConville, J. B., Neill, D. J., and McNally, P. J., "System Level Dynamic Aeroelastic Simulation: Store Separation in MSC.ADAMS Using Quasi-static, Higher Order Potential Aerodynamics," *Aerospace Flutter and Dynamics Council*, Dayton, OH, May 7-9, 2003.

[4]Love, H.H, Zink, P.S., Stroud, R.L., Bye, D.R., Chase, C., "Impact of Actuation Concepts on Morphing Aircraft Structures", AIAA 2004-1724, *45th AIAA/ASME/ASCE/AHS/ASC Structures, Structural Dynamics & Materials Conference*, Palm Springs, California, 19-22 April 2004.

[5]Scarlett, J. N., Canfield, R. A., and Sanders, B., "Multibody Dynamic Aeroelastic Simulation of a Folding Wing Aircraft," AIAA 2006-2135, *14th AIAA Adaptive Structures Conference*, Newport, RI, May 1-4, 2006.

[6]Rodden, W. P. and Johnson, E. H., "MSC/NASTRAN User's Guide: Aeroelastic Analysis," Macneal-Schwendler Corporation, Los Angeles, CA, 1994.

[7]Neill, D. J., Herendeen, D. L., and Venkayya, V. B., "ASTROS Enhancements: Volume III – ASTROS Theoretical Manual," WL-TR-95-3006, Air Force Wright Laboratory, WPAFB, OH, April 1995.

[8]Doman, D. B. and Oppenheimer, M. W., "Reconfigurable Control Design for the X-40A with In-Flight Simulation Results," AIAA 2004-5017, *AIAA Guidance, Navigation, and Control Conference*, Providence, Rhode Island, 16 - 19 August 2004.

Development of Next-Generation Morphing Aircraft Structures

Jason Bowman[***], Brian Sanders[†††], Bryan Cannon[‡‡‡]
Air Force Research Laboratory, Wright-Patterson Air Force Base, OH 45433

Jayanth Kudva[§§§] and Shiv Joshi[****]
NextGen Aeronautics, Inc., Torrance, CA 90505

Terrance Weisshaar[††††]
Purdue University, West Lafayette, IN, 47907-2023

This p aper presents a n o verview o f t he w ork p erformed u nder t he DARPA/AFRL/NextGen Morphing Aircraft Structures (N-MAS) program and in-house Air Force R esearch L aboratory ef forts i ncluding be nefits o f s hape m orphing, e volution, development, a nd key f eatures o f t he de sign, a pproach t o s tructural i ntegrity a nd w ind tunnel testing, and key challenges and future plans to develop operational morphing UAVs.

I. Introduction

The past decade of adaptive structures and smart materials technology development has progressed from simple component technology demonstrations to integrated systems on flight-traceable structures. Of interest here are technologies and concepts which enable large shape changes on aircraft. The goal of shape change is not an end unto itself, but rather a means to expand the performance capabilities of aircraft. Such large shape changes are commonly referred to as aircraft morphing. In particular, morphing wings, defined as wings that undergo very large changes in geometry (span, area, chord, sweep, etc.) such that the wing configuration is optimized for widely varying flight conditions (e.g., loiter, dash, and high-speed maneuvers), have the potential to revolutionize future designs of military and possibly commercial aircraft.

Although morphing is a recent aeronautical term that describes these relatively new technologies, in a general sense it describes changes in vehicle state and shape. In the broadest sense of the term, shape morphing has been used with ever-increasing effectiveness since the Wright brothers. For instance, changing wing camber by twisting the wing as the Wright brothers did, or using control surfaces as almost all aircraft do to this day, can be construed to be shape morphing to enable improved performance at different flight conditions – maneuver, take-off, high angle of attack, etc. As a further example, a retractable landing gear alters the shape of the aircraft to reduce drag during flight. And perhaps the most effective implementation of shape morphing is variable sweep wings as exemplified by the F-111, B-1, and F-14 aircraft.

Having just completed a major program to test morphing technologies and concepts in a wind tunnel under realistic loads, with new programs to study morphing flight and actuator control, and an identified need for better unmanned vehicles in the next decade, this paper addresses three important aspects of the problem – reasons to morph, technology and system development at NextGen Aeronautics to increase the technology readiness level (TRL) of morphing, and future work required to address technology maturation, technology transition and system integration challenges.

Companion papers in this conference provide details on the work done at NextGen under the N-MAS and related programs including: morphing wing concepts and design development [1]; actuation system design, fabrication and

---

testing of a the morphing wing wind tunnel model [2]; wind tunnel test results [3]; aeroelastic analysis of the morphing wing [4]; development and testing of the jet-powered NextGen morphing demonstrator UAV, the MFX-1 [5]; and intelligent control of a morphing aircraft [6].

II. The Benefits of Morphing

Morphing, like any other technology, has to demonstrate system level performance benefits prior to implementation on an aircraft. If one can imagine various system functions as expanding circles on a Venn diagram, the goal over time is to expand those capabilities with technology so that a desired level of overlap exists. The goal is to use shape change to reduce the level of compromise in the aerodynamic and propulsive functions of the vehicle. The effect is expanded flight envelopes and perhaps the ability of one vehicle to do the job of many (Figure 1).
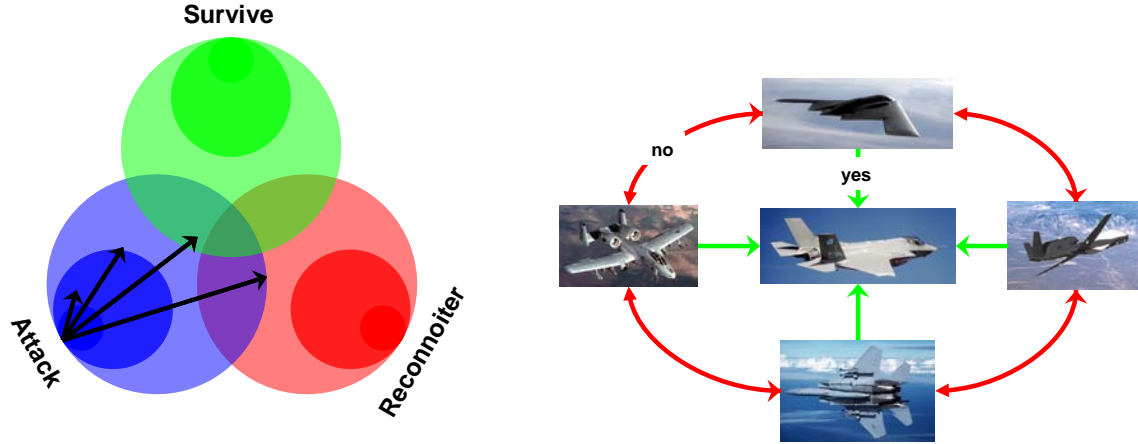

Figure 1. Capability vs. Time

First-Order Assessment of Morphing Benefits: Variable sweep aircraft being the current state-of-the-art in shape changing wings, the next step in morphing is to implement large changes in wing geometric parameters including sweep, span, chord and aspect ratio – such changes are required to provide revolutionary improvements in system level performance. Under Phase 1 of the N-MAS program (Jan 2003 – Jan 2004), the NextGen team conducted a first order study to assess the potential benefits of wing morphing. The results of this study in terms of system-level performance improvements, based on the NextGen design, are illustrated in the spider plot in Figure 2. Flight performances, based on first order calculations, are also shown for fixed and morphing wing geometries. The outermost points represent the theoretically best performance at each of the designated flight conditions. It should be noted that variable sweep is a subset of the NextGen design. A couple of points to note: (1) these results are based on particular fixed-wing baseline aircraft with the morphing wing design subject to reasonable and realistic geometric constraints; and (2) while the exact values of the improved performance shown in the figure are based on text-book formulas, and are indeed indicative of potential benefits, the figure is meant to be illustrative and not definitive; as a matter-of-fact, the entire N-MAS team, found this to be sufficient rationale for progress on developing of a wind-tunnel and flight model.
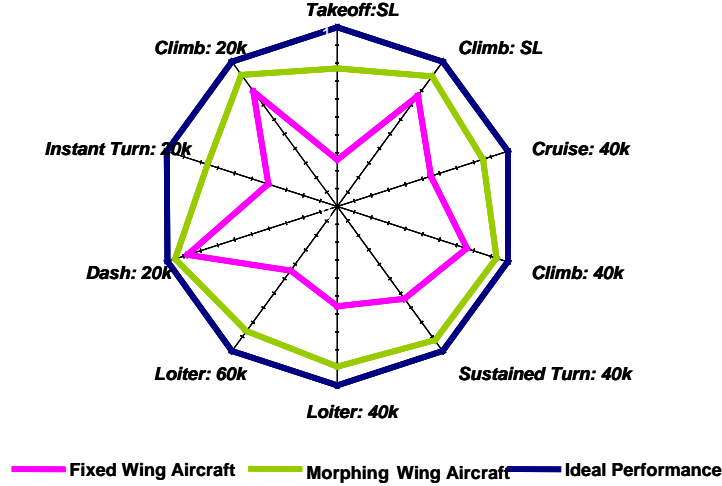
24

Figure 2. Spider plot comparison of fixed and morphing wing aircraft

Hunter-Killer as an Example Mission: Another way of demonstrating the benefits of morphing are at the low-level metrics such as lift-to-drag ratio and relate them to system-level metrics which include life cycle cost, flyaway cost, cost per kill box, and percent of red killed, to name a few. The main issue is that the mappings are not usually linear or sometimes even discontinuous from lower to higher levels of metrics.

With this in mind, the following analysis is one example of marching from lower to one particular higher level metric, number of sorties, for a time-sensitive target (TST) hunter-killer mission. By its nature, this analysis, which is fuel based, does not addresses other benefits of morphing such as improved point performance (turn rate, takeoff distance, etc.) or primary flight control.

For fuel-based metrics, the primary driver is the vehicle lift-to-drag ratio, which is driven by lift and drag coefficients, and specific fuel consumption. Although morphing is being applied to engine cycles in other technology programs in AFRL, the concentration here will be strictly on the aerodynamics of the vehicle. A basic subsonic drag polar can be expressed as

$$C_D = C_{D_p} + k\left(C_L - C_{L_0}\right)^2 \tag{1}$$

There are various optimal points in the drag polar defined by maximizing $C_L^{3/2}\big/C_D$, $C_L\big/C_D$, or $C_L^{1/2}\big/C_D$. Since lift coefficient is influenced by wing loading, altitude, and flight speed, wing loading is often a compromise based on the assumed flight conditions. Aspect ratio and wing camber are also compromises since they influence the value of k and C_{L_0}, respectively. The fuel efficiency potential of morphing can be immediately seen as the ability to adjust the wing area, aspect ratio, and camber such that the vehicle is flying at or near the optimal lift coefficient most of the time. If transonic and supersonic conditions are also considered, then sweep and wing thickness also come into play.

A successful example of sweep and camber change was demonstrated in the AFRL supported "Mission Adaptive Wing" program [7]; also an optimization procedure using "Morphing as an Independent Variable" to find the optimal vehicle geometry as a function of mission leg was demonstrated in References 8 and 9. The latter represents an extension and formalization of what is already done in design, which is to decide whether a particular technology or suite of technologies is worth implementing.

If morphing did not have a weight or cost penalty, then morphing would always make sense. But now consider a non-morphing aircraft (interchangeably referred to as a fixed wing aircraft here) in a mission where most of the fuel is burned at one flight condition. An optimizer will select a vehicle configured for that flight condition with some compromise for the other flight conditions. Even if fuel efficiency is very low during a leg, if that leg is very short the actual fuel wasted is small compared to the rest of the mission, and the effect on the system due to the low efficiency is negligible. For a morpher with a weight penalty, it is clear that there is a cross over point where fuel penalties for not morphing begin to exceed the morphing weight penalty. The one criterion clearly evident from the definition of lift coefficient for morphing to be beneficial is a large difference in dynamic pressure over at least two mission legs for extended periods of time. The ideal case for a morphing aircraft is where a large difference in

25

dynamic pressure exists and the fuel fractions (not time) for those two legs are equal. For such missions, it is conceivable that there is no feasible non-morphing solution. Another good, though not perfect, indicator for morphing is to look at designs where requirements have been relaxed in order to find a closed solution for a non-morphing system.

To begin to understand how improvements in lift-to-drag ratio and morphing weight penalties affect the higher level metrics, a hunter-killer mission is examined with number of sorties as the metric. In this mission, time-sensitive targets (TSTs) present themselves for short periods of time to attack friendly forces and then disappear. This mission exercises both loiter (hunting) and dash capabilities (to reach a target within weapons range before the TSTs disappear).

One traditional method for examining the trade space of attack missions is to understand the relationship between combat zone radius (CZR) and total mission radius (TMR). When converted to time, results for a series of runs can be seen in Figure 3. Points that line up along the diagonal are essentially all dash (no loiter) if the out and back cruise times are not considered. The x-axis represents an all-cruise or all-loiter mission. Blue dots indicate a hunt-and-kill mission; green dots indicate a hunt (ISR) mission with a combat air patrol (CAP) aircraft primarily doing the killing.
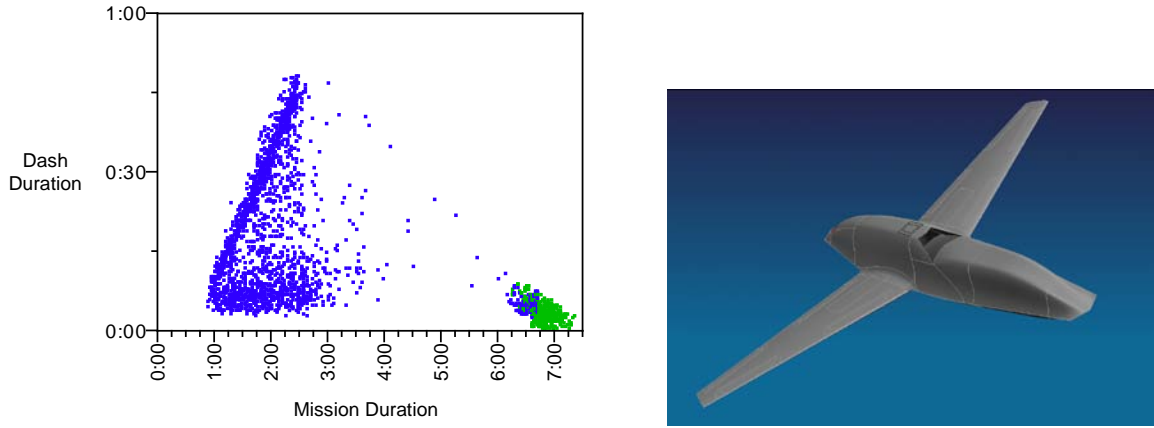

Figure 3. Typical TST Hunter-Killer Mission and Optimized Non-Morphing Platform

Notice that many sorties have relatively significant amounts of dash relative to loiter if the cruise times are not considered. This is a result of the sensor capability. The more quickly targets are found the less loitering is done. If one defines a kill-to-hunt ratio $\overline{t_D} \equiv t_D/t_L$, this ratio is about 0.5 on average along the diagonal. This ratio will be seen to be an important criterion for determining if morphing is beneficial for this mission. But this data taken in its entirety certainly indicates that a hunter-killer mission is cruise- and loiter-dominated. Previous in-house studies at AFRL have shown that for a loiter-dominated mission with a dash constraint, an optimizer will select medium to medium-high aspect ratios with medium sweep angles as shown in Figure 3.

To understand the impact of this kill-to-hunt distribution from a theoretical point of view, consider a basic sizing expression with a penalty factor f_{W_e} on empty weight, which is a linear function of gross weight $W_{empty} = f_{W_e}(mW_0 + b)$.

$$W_0 = \frac{f_{W_e}b + W_{payload}}{\beta - f_{W_e}m} \quad (2)$$

β is the product of the Breguet range (cruise and dash) and endurance expressions. Using eq. 2, it can be shown that for two vehicles where vehicle (1) is a reference and vehicle (2) has improved performance but an empty weight penalty, the ratio of loiter times is approximately

$$\frac{\sum t_L^{(2)}}{\sum t_L^{(1)}} = f_{t_L} = \frac{f_{E_L}}{f_{SFC_L}}\left(1 + \Delta_C + \Delta_D - e\right) \quad (3)$$

where

$$\Delta_C = \frac{E_L}{E_C}\frac{SFC_C}{SFC_L}\left(1 - \frac{f_{SFC_C}}{f_{E_C}}\frac{\sum t_C^{(2)}}{\sum t_C^{(1)}}\right)\left(\frac{\sum t_C}{\sum t_L}\right) \qquad \Delta_D = \frac{E_L}{E_D}\frac{SFC_D}{SFC_L}\left(1 - \frac{f_{SFC_D}}{f_{E_D}}\frac{\sum t_D^{(2)}}{\sum t_D^{(1)}}\right)\left(\frac{\sum t_D}{\sum t_L}\right)$$

$$e = \left(\frac{E_L}{SFC_L\sum t_L}\right)\left[\ln a + m\left(\frac{f_{W_E}}{a} - 1\right)\right] \qquad a = \frac{f_{W_e}\,{b}/{W_{payload}} + 1}{{b}/{W_{payload}} + 1}$$

Values of ${b}/{W_{payload}}$ are typically about 0.1. The cruise and dash increments Δ_C and Δ_D illustrate the effect of improvements in lift-to-drag ratio f_E (the ratio of lift-to-drag ratios due to technology improvement) and specific fuel consumption f_{SFC} on loiter time while the last term e describes the decrease in loiter time due to weight penalties. Note that the more efficient the reference vehicle is, the higher the penalty. If there is little room for improvement but weight is being added, then the relationship indicates that is not a good choice. Note that changes in L/D and SFC or the weight penalty do not have morphing-specific influence, which makes these relationships valid for any technology.

If the cruise and dash times are held constant between the two vehicles, then it is easy to observe that mission parameters are just as influential as the technology parameters in influencing loiter time. These mission parameters are the cruise-to-loiter $\overline{t_C} \equiv \dfrac{\sum t_C}{\sum t_L}$ and dash-to-loiter (kill-to-hunt) $\overline{t_D} \equiv \dfrac{\sum t_D}{\sum t_L}$ time ratios. One must not interpret that increased cruise-to-loiter or dash-to-loiter times improve loiter time. The relationship simply says that if these ratios are high, the room for improvement in loiter time is larger if technology can impact L/D and SFC. These relationships allow designers to quickly determine where the cross over point is for morphing. To illustrate the effect, quick estimates of some of the parameters are presented in Table 1.

Table 1. Estimated Values of Flight Parameters

Parameter	Description	Value
E_L/E_D	Ratio of loiter and dash lift-to-drag ratios	3
f_{E_D}	Improvement in dash L/D (E)	1.2
f_{E_L}	Improvement in loiter L/D (E)	1.1
m	Sensitivity of empty weight to gross weight	0.55
$b/W_{payload}$	No interpretation, but usually around 10%	0.1
t_L, E_L, SFC_L	Loiter time, L/D, and SFC	5 hr, 15, and 0.8 per hr

The improvement in loiter time for various kill-to-hunter ratios and empty weight penalties is shown in Figure 4. If the empty weight penalty is conservatively set at 10%, then the cross over point for morphing is about $\overline{t_D} = 0.25$. Therefore a relatively large number of sorties must exceed this value for morphing to make sense.
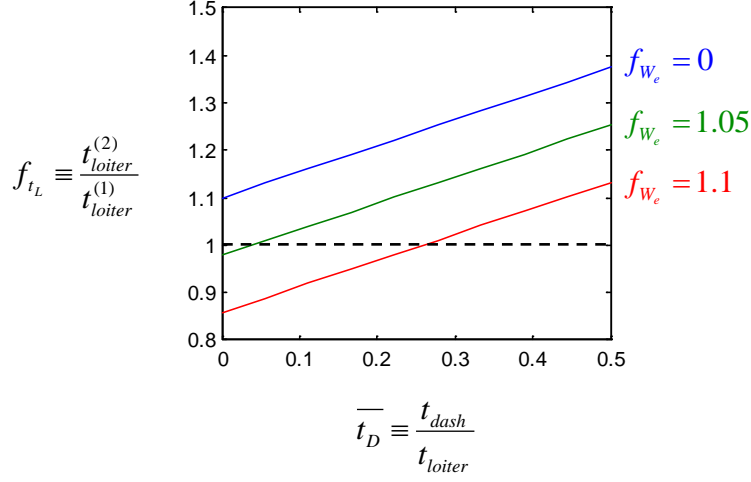
$$f_{t_L} \equiv \frac{t_{loiter}^{(2)}}{t_{loiter}^{(1)}}$$

$$\overline{t_D} \equiv \frac{t_{dash}}{t_{loiter}}$$

Figure 4. Improvement in Loiter Time Due to Morphing for Various Missions

Consider an approximate theoretical expression for the number of sorties, shown as a ratio of aircraft (2) sorties to aircraft (1) sorties, and fleet size N (UR is the utilization rate).

$$\frac{S_2}{S_1} \approx \frac{1 + \overline{t_C} + \overline{t_D}}{f_{t_L} + \overline{t_C} + \overline{t_D}} \qquad N = ceil\left[\frac{1}{UR}\left(1 + \frac{\overline{t_C}}{f_{t_L} + \overline{t_D}} \right) + 1 \right] \tag{4}$$

The largest reduction in sorties is realized when the cruise and dash time are relative small compared to loiter. But for typical values $\overline{t_C} = 0.3$ and $\overline{t_D} = 0.25$ and $f_{t_L} = 1.25$, the sortie rate is decreased by 15%. Reductions of 20% or more would not be out of the question for other missions. But the fleet size is not affected at all for reasonable improvements in loiter time except when the basing distanced is large making $\overline{t_C}$ large.

Examining simulation results in Figure 5 for the number of sorties required for non-morphers and morphers, the theoretical sortie ratio expression is fairly accurate. One interesting trend that can be seen in Figure 5 is that sortie rate is only a function of gross weight under 20,000 lbs gross weight. For the non-morpher above 20,000 lbs, sortie rate is also a function of the search radius. This is because vehicles under 20,000 lbs are very fuel constrained. To carry a sufficient number of weapons means that the fuel fraction decreases with decreasing vehicle size. Above 20,000 lbs where fuel to fly "overhead" (cruise out and cruise back) is no longer constraining, the solution is more sensitive to the operational parameters of interest such as search radius.
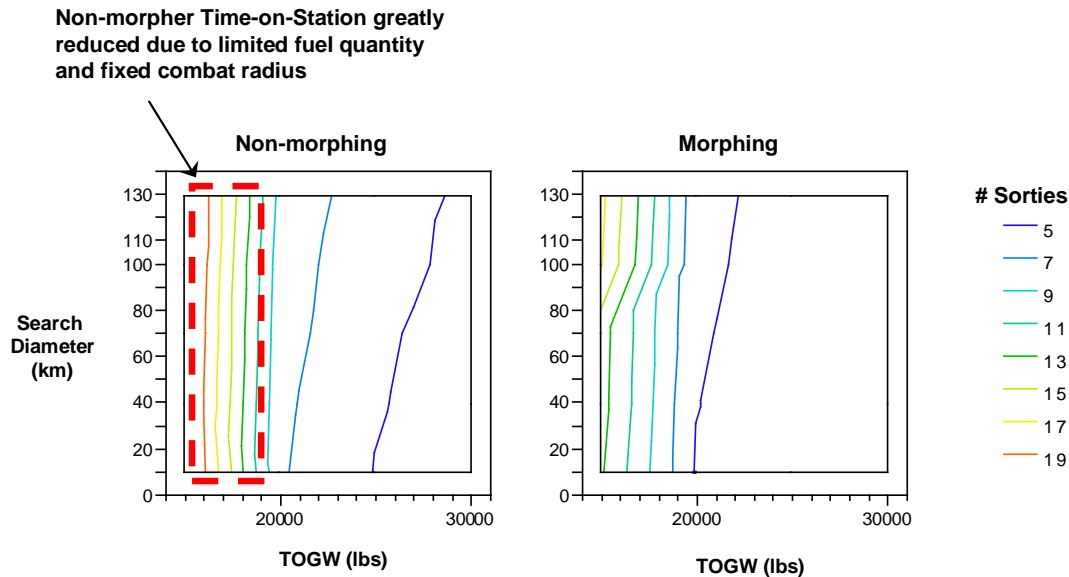
Figure 5. Number of Sorties for Non-Morphing (left) and Morphing (right)

Although trade spaces such as those shown for sortie rate contain useful information, statistical techniques can be applied to the data to find clear trend information. Classification and Regression Tree (CART) analysis organizes the data in a format more useful for decision making. CART analysis classifies data at multiple hierarchal levels. The best way to explain this is with a morphing example (Figure 6).
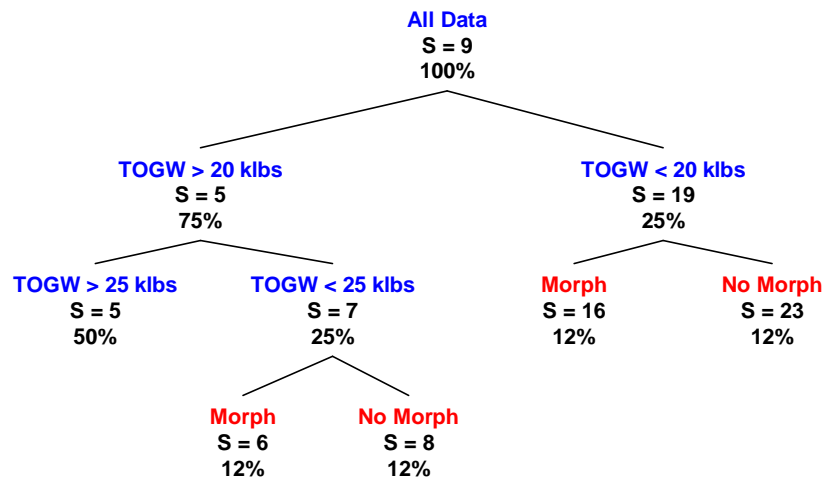

Figure 6. CART Analysis Based for # of Sorties Based on Gross Weight and Morphing

When CART is applied to the hunter-killer sortie data, gross weight is by far the most important effect; the larger the vehicle the larger the fuel fraction for a fixed number of weapons. Vehicles under 20,000 lbs have a mean sortie rate of 19, and vehicles above 20,000 lbs have a mean sortie rate of 5 clearly showing the effect of fuel fraction. The CART analysis also makes it clear that when the vehicle is under 20,000 lbs, it pays to morph with a sortie rate of 15 compared to a non-morpher sortie rate of 22, which is a 30% reduction in sortie rate! For weights between 20,000 lbs and 25,000 lbs, morphing also has an influence on sortie rate, but this effect is lower on the tree than the main effect of gross weight.

The conclusion for a hunter-killer mission is that morphing does make sense (even with a 10% empty weight penalty), especially for vehicles under 20,000 lbs. If the mission was made harder by increasing the basing distance or search radius, this break point in vehicle weight would also increase.

Are there other missions or reasons to morph? Reference 8 shows that morphing has a large impact on fleet size for a Coast Guard patrol mission. The key to morphing for this mission is a high altitude cruise out to station with fast response time then a low altitude, slow patrol. For the hunter-killer mission, there may also be a requirement for maneuverability, although this is uncertain. Being able to rapidly reconfigure from the loiter configuration to a more maneuverable configuration with higher g-force capability gives maneuverability without a large increase in wing weight. Work in morphing flight controls also shows that morphing degrees-of-freedom can be taken advantage of for primary flight control [6].

III. Overview of the NMAS Program

The NMAS program, initiated in January 2003, had a tight 36-month schedule. During the first three months, over 20 different concepts including telescoping wings, joined wings, and fan wings were generated by the team, guided primarily by the requirement to realize large geometry changes. These concepts were downselected to three final candidates using a modified Pugh method. From these a final design, termed the 'batwing,' was chosen based on the following criteria: overall performance, actuation power requirement estimates, perceived ease of manufacture, and feasibility of designing, fabricating and testing a wind tunnel model within program budget and schedule constraints.

The NextGen design is capable of large geometry changes including 200% change in aspect ratio, 40% in span and 70% in wing area; further, within reasonable limits, these can be tailored for specific performance and design requirements. Figure 7 shows the nominal configurations of the NextGen design for five specific flight conditions. Key innovations of the design include: (1) a two degree-of-freedom system which enables independent control of wing sweep and wing area; (2) a novel flexible skin design which can undergo over 100% in-plane strain while withstanding air loads of up to 400 psf; (3) an actuation system consisting of multiple internal actuators, centrally computer controlled to implement any commanded morphing configuration; and (4) a structurally efficient, kinematic substructure which enables the morphing geometry changes.

Figure 7. Morphing wing configurations for high-lift, climb, cruise, loiter, and maneuver

Development of the revolutionary batwing concept required an unconventional approach since not only are appropriate design and analysis tools unavailable, even the procedures and methods to be used to guide the development are not clear. For instance, the flexible skin required low in-plane stiffness to permit in-plane morphing but high flexural stiffness to withstand normal air loads. To address such challenges and circumvent the limitations, the NextGen team resorted to an iterative and ad hoc design-analysis-test approach. The final skin design, a macro-composite with multi-directional reinforcements, resulted from testing the subcomponents separately and jointly. Analytical modeling using both empirical approaches and finite element analyses guided the testing and design evolution. Other challenges similarly addressed include: providing sufficient torsional stiffness in the overall structure since the flex-skins design essentially eliminated a conventional wing torque-box; ensuring adequate flutter and divergence margins in a wing consisting of components with widely varying stiffnesses; developing an efficient kinematic sub‐structure and modeling the internal joints to obtain accurate predictions of internal loads and stresses; and incorporating multiple actuators within the limited internal space and controlling them so as to provide efficient and reliable morphing changes.

A wind tunnel model of the batwing design (Figure 8) with the following features was fabricated: total weight = ~1200 lbs; wing sweep variable from 15 to 45 degrees; wing area variable from 15 sq-ft to 24 sq-ft; and half-span variable from 7 to 10 ft. The model consisted of rigid leading and trailing edges and wing tip, with a kinematic midsection attached to top and bottom flexible skins. An innovative two degree-of-freedom root joint provided independent control of the wing sweep and wing area. The actuation system consisted of nine separate hydraulic actuators centrally controlled provided efficient and coordinate control of the wing geometry.

Figure 8. Batwing model in the NASA Langley TDT wind tunnel

Wind tunnel testing was performed at the NASA Langley Transonic Dynamic Tunnel (TDT) over a three week period in October/November 2005. Over 25 hours of testing was performed at Mach numbers varying from 0.2 to 0.92 and operating conditions representative of altitudes varying from sea level to 50,000 ft. The main objectives of the wind tunnel testing was to: establish the structural integrity of the overall design by testing at up to 2.5g loads, demonstrate controlled morphing at 1-g air-on conditions, and correlate analytical predictions with measured results. All these objectives were successfully met. Additionally, as a proof-of-concept demonstration, the NextGen team developed and successfully flight tested a 100 lb, jet-powered RC UAV, termed the MFX-1. This flight test included the first ever demonstration of in-flight morphing.

Companion papers in this session address specific aspects of the program including concept development and design, aeroelastic analysis, fabrication process, wind tunnel testing, and the MFX-1 flight test [1-6].

The N-MAS program has provided a strong foundation to proceed towards the development of an operational transonic morphing wing UAV which will provide multi-role capabilities, hitherto achievable only using multiple aircraft.

IV.   Future of Morphing

Like all new technologies, the future of morphing is uncertain. Technology programs (beyond basic research) need to be matched to capability gaps to ensure relevance and funding. Morphing does show promise for several types of missions, but to say there is a compelling case for morphing is perhaps an overstatement. Like many of the technologies that are now taken for granted, perhaps morphing should be viewed as a matter of practicality as a design option. If it makes sense for the particular application, then use it. If it does not make sense, then that is acceptable, too.

Morphing as a suite of technologies is not flight ready. Much work is needed in its component technologies such as skins, actuators, mechanisms, and control theory (primary flight and actuation) for morphing to be truly realized. AFRL has done control theory work through two SBIR programs. One program studied actuation control, and the other studied how to take advantage of the morphing degree-of-freedom for primary flight control rather than just accomodating it. More information can be found in Reference 6. Flight control of bird-size morphing vehicles capable of asymmetric wing positions is also being studied to understand what advantages morphing affords at that scale [10].

Morphing design tools and methods are also required to ensure the success of morphing. Work done in Reference 11 illustrated the inability of current structural design tools to accodomodate the morphing degree-of-freedom very well. The basic issue is one of serial optimization of "snap shots" of the morphing design or simultaneous design and optimization of the morphing design. AFRL and others have been addressing topology optimization of adaptive wings to understand the mechanisms required to achieve desired shapes [12]. AFRL has also taken the next step of establishing algorithms to design theoretical skins with tailored properties to achieve the desired flexibility in one direction and stiffness in other directions in an iterative process with the mechanism topology optimization. Recognizing that design interactions are more problematic with morphing vehicles, AFRL devleoped an engineering simulation framework capable of analyzing the interactions between the structure,

mechanism, aerodynamics, and primary flight control algorithms of the vehicle [13]. Finally, work needs to be done on aircraft sizing tools. Hypersonics, morphing, and energy/exergy-based analysis are all examples that have shown the limitations of current sizing tools such as FLOPS. Approaches such as those taken in References 8, 9, and 14 need to be taken a step further and a generalized, user-extensible framework developed.

But for all of these efforts to pay off, the morphing technology needs a transition program in order for aerospace community to take the the technology seriously and have it as a design option. While morphing on vehicles exceeding several thousand pounds gross weight may not be practical in the near term due to the technology readiness levels, it is generally acknowledged that a good first opportunity is on smaller unmanned aircraft or missiles where current or near-term technology can be applied to achieve morphing.

V. Summary

Morphing is currently at a cross roads where much of the requisite initial work has been completed but much hard work remains. Basic morphing benefits and procedures for identifying likely mission applications have been developed, and the basic technology and flight-traceable system integration programs have been completed. The NMAS experience has been presented here to illustrate the flight-traceable integration aspect.

The next steps for morphing are clear but require an impetus such as a demonstrator program to provide direction. In the mean time, many organizations continue to develop design tools and procedures for developing and analyzing the morphing problem in all respects including aerodynamics, structures and mechanisms, skins, actuation, and flight control.

References

1. S. Joshi, A. Jha, J. Rodrian, R. Alphenaar, K. and Szema, "Design of the NextGen Morphing Wing Wind Tunnel Model," *AIAA SDM Conference*, xxxxx, AIAA, Honolulu, HI, 2007.

2. C. Hebert, M. West, and B. Cannon, "Actuation System Design, Fabrication, and Testing for a Morphing Wing Structure," *AIAA SDM Conference*, xxxxx, AIAA, Honolulu, HI, 2007.

3. R. Strutzenberg, M. Scott, C. Wieseman, and D. Piatak, "Wind Tunnel Test and Results of NextGen Morphing Wind Tunnel Model," *AIAA SDM Conference*, xxxxx, AIAA, Honolulu, HI, 2007.

4. G. Andersen, D. Cowan, and D. Piatak, "Aeroelastic Modeling, Analysis, and testing of a Morphing Wing Structure," *AIAA SDM Conference*, xxxxx, AIAA, Honolulu, HI, 2007.

5. J. Flanagan, "Development and Flight Testing of a Morphing Aircraft, the NextGen MFX-1," *AIAA SDM Conference*, xxxxx, AIAA, Honolulu, HI, 2007.

6. N. Gandhi, A. Jha, T. Seigler, J. Monaco, D. Ward, D. Inman, and D. Howard, "Intelligent Control of a Morphing Aircraft," *AIAA SDM Conference*, xxxxx, AIAA, Honolulu, HI, 2007.

7. "AFTI/F-111 Mission Adaptive Wing Briefing to Industry". AFWAL-TR-88-3082. October 1988.

8. B. Roth, C. Peters, W. Crossley, "Aircraft Sizing with Morphing as an Independent Variable: Motivation, Stategies, and Investigations". AIAA 2002-5840. AIAA's Aircraft Technology, Integration, and Operations (ATIO) 2002 Conference. 1-3 Oct 2002. Los Angeles, CA.

9. J. Frommer, W. Crossley, "Building Surrogate Models for Capability-Based Evaluation: Comparing Morphing and Fixed Geometry Aircraft in a Fleet Context.". AIAA 2006-7700. 6th AIAA Aviation Technology, Integration, and Operations Conference (ATIO). 25-27 September 2006, Wichita, Kansas.

10. D. Grant, M. Abdulrahim, R. Lind, "Flight Dynamics of a Morphing Aircraft Utilizing Independent Multiple-Joint Wing Sweep". AIAA 2006-6505. AIAA Atmospheric Flight Mechanics Conference and Exhibit. 21-24 August 2006. Keystone, CO.

11. M. Snyder, B. Sanders, F. Eastep, G. Frank, "Vibration and Flutter Characterisitcs of a Folding Wing". AIAA 2005-1994. 46th AIAA/ASME/ASCE/AHS/ASC Structures, Structural Dynamics & Materials Conference. 18-21 April 2005, Austin, TX.

12. K. Maute, G. Reich, "Integrated Multidisciplinary Topology Optimization Approach to Adaptive Wing Design". Journal of Aircraft. Vol 43, No. 1, January-February 2006.

13. J. Bowman, G. Reich, B. Sanders, "Simulation Tool for Analyzing Complex Shape-Changing Mechanism in Aircraft". AIAA Modeling and Simulation Technologies Conference and Exhibit. 21-24 August 2006. Keystone, CO.

14. T. Nam, D. Soban, D. Mavris, "A Generalized Aircraft Sizing Method and Application to Electric Aircraft". AIAA 2005-5574. 3rd International Energy Conversion Engineering Conference. 15-18 August 2005. San Fransisco, CA.